LEBANESE AMERICAN UNIVERSITY

Effect of SLC35b4 Knockdown on Total and O-Glycosylated Cellular Proteins in HepG2 Cell Line

By

Gregory Antonios

A thesis
Submitted in partial fulfillment of the requirements
for the degree of Master of Science in Molecular Biology

School of Arts and Sciences
September 2012

Thesis Proposal Form

LAU
الجامعة اللبنانية الأميركية
Lebanese American University

Lebanese American University
School of Arts and Sciences - Byblos Campus

Thesis Proposal Form

Name of Student: Gregory Antonios I.D.#: 200904351

Program / Department: Molecular Biology M.S. / Department of Natural Sciences

On (dd/mm/yy): Has presented a Thesis proposal entitled:

Effect of Solute Receptor *SLC35b4* on cellular O-Glycosylation and its association with glucose production

In the presence of the Committee Members and Thesis Advisor:

Advisor: Dr. Brigitte Wex [redacted]
(Name and Signature)

Committee Member: Dr. Soha Yazbek [redacted]
(Name and Signature)

Committee Member: Dr. Sima Tokajian [redacted]
(Name and Signature)

Comments / Remarks / Conditions to Proposal Approval:

Date: 21.5.12 Acknowledged by [redacted]
(Dea iences)

cc: Department Chair
Thesis Advisor
Student
School Dean

Thesis Defense Result Form

LAU
الجامعة اللبنانية الأميركية
Lebanese American University

Lebanese American University
School of Arts and Sciences - Byblos Campus

Thesis Defense Result Form

Name of Student: Gregory Antonios I.D.: 200904351
Program / Department: Molecular Biology M.S. / Department of Natural Sciences
Date of thesis defense: 21/9/2012
Thesis title: Effect of SLC35b4 knockdown on Total and O-glycosylated Cellular Proteins in HepG2 Cell Line

Result of Thesis defense:

☑ Thesis was successfully defended. Passing grade is granted

☐ Thesis is approved pending corrections. Passing grade to be granted upon review and approval by thesis Advisor

☐ Thesis is not approved. Grade NP is recorded

Committee Members:

Advisor: Dr. Brigitte Wex [redacted]
(Name and Signature)

Committee Member: Dr. Soha Yazbek [redacted]
(Name and Signature)

Committee Member: Dr. Sima Tokajia [redacted]
(Name and Signature)

Advisor's report on completion of corrections (if any):

Changes Approved by Thesis Advisor: BRIGITTE WEX Signature: [redacted]

Date: 25.09.2012 Acknowledged by [redacted]
(Dean, School of Arts and Sciences)

cc: Registrar, Dean, Chair, Advisor, Student

Thesis Approval Form

Lebanese American University
School of Arts and Sciences - Byblos Campus

Thesis Approval Form

Student Name: Gregory Antonios I.D. #: 200904351

Thesis Title: Effect of SLC35b4 Knockdown on Total and O-Glycosylated Cellular Proteins in HepG2 Cell Line

Program / Department: Molecular Biology M.S. / Department of Natural Sciences

School of Arts and Sciences

Approved by:

Thesis Advisor: Dr. Brigitte Wex

Committee Member: Dr. Soha Yazbek [redacted]

Committee Member: Dr. Sima Tokjian

Date 21st September, 2012

THESIS COPYRIGHT RELEASE FORM

LEBANESE AMERICAN UNIVERSITY NON-EXCLUSIVE DISTRIBUTION LICENSE

By signing and submitting this license, you (the author(s) or copyright owner) grants to Lebanese American University (LAU) the non-exclusive right to reproduce, translate (as defined below), and/or distribute your submission (including the abstract) worldwide in print and electronic format and in any medium, including but not limited to audio or video. You agree that LAU may, without changing the content, translate the submission to any medium or format for the purpose of preservation. You also agree that LAU may keep more than one copy of this submission for purposes of security, backup and preservation. You represent that the submission is your original work, and that you have the right to grant the rights contained in this license. You also represent that your submission does not, to the best of your knowledge, infringe upon anyone's copyright. If the submission contains material for which you do not hold copyright, you represent that you have obtained the unrestricted permission of the copyright owner to grant LAU the rights required by this license, and that such third-party owned material is clearly identified and acknowledged within the text or content of the submission. IF THE SUBMISSION IS BASED UPON WORK THAT HAS BEEN SPONSORED OR SUPPORTED BY AN AGENCY OR ORGANIZATION OTHER THAN LAU, YOU REPRESENT THAT YOU HAVE FULFILLED ANY RIGHT OF REVIEW OR OTHER OBLIGATIONS REQUIRED BY SUCH CONTRACT OR AGREEMENT. LAU will clearly identify your name(s) as the author(s) or owner(s) of the submission, and will not make any alteration, other than as allowed by this license, to your submission.

Gregory Antonios

Signature: 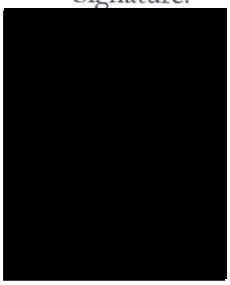

Date: 21-September-2012

PLAGIARISM POLICY COMPLIANCE STATEMENT

I certify that I have read and understood LAU's Plagiarism Policy. I understand that failure to comply with this Policy can lead to academic and disciplinary actions against me.

This work is substantially my own, and to the extent that any part of this work is not my own I have indicated that by acknowledging its sources.

Gregory Antonios

Signature: [redacted] Date: 21-September-2012

ACKNOWLEDGMENTS

I'm grateful to *some* people at the Lebanese American University who have made all this work possible. *First* and *foremost*, my thanks go to Ms. Maya Farah; for going above and beyond the call of duty for all of us graduate students. My deepest gratitude goes to Dr. Brigitte Wex for being an advisor in the truest sense of the word. Many thanks are due to Dr. Sima Tokajian who was part of my thesis committee and has done all in her power to support me. I'm also grateful to Dr. Costantine Daher, chairperson of the Natural Sciences department, for steering a ship while the storm is raging.

A special heartfelt gratitude is to Prof. Fouad Hashwa who has made an enormous contribution to my future.

I am appreciative of Dr. Soha Yazbek's guidance in what was a continuation of her work and ideas and wish to thank her for the opportunity she gave me to work at the American University of Beirut Medical Center.

A special thanks to Mr. Khalil Kreidieh who was my officemate at AUB and was a tremendous help with the work that was done there.

To my brother from another mother, Sami Yammine, because he is a pillar in my life; may the days to come bring us only life.

To my brother from the same mother, Joe El- Khoury, because I'm sure life will re-unite us some way, somehow.

Gregory Antonios

To Nadim, our Pillar..

To Therese, the Cornerstone..

To Anna, the dough which I have molded..

To Mady, our Northern Star..

And

To Poush, the Purest of all.

Effect of SLC35b4 Knockdown on Total and O-Glycosylated Cellular Proteins in HepG2 Cell Line

Gregory Antonios

Abstract

Diabetes is considered a Non-Communicable Disease (NCD). Type II diabetes is caused by the lack of insulin production from liver beta cells in the aftermath of insulin resistance. Slc35b4 encodes a protein that transports UDP-xylose and UDP-N-acetylglucosamine from the cytosol into the golgi. UDP-N-acetylglucosamine then serves as both a substrate for O-linked glycosylation (O-GlcNAC) and as a negative feedback inhibitor of the Hexosamine Biosynthesis Pathway (HBP) pathway. Solute receptor SLC35b4 has been identified, using both genetic and functional studies, as a regulator of obesity, insulin resistance and gluconeogenesis by Yazbek *et al.* Over 600 proteins are modified with the addition of an O-GlcNAC moiety and may therefore contribute to the phenotype. This study employs One Dimensional (1D) and Two Dimensional (2D) electrophoresis to investigate differentially expressed O-glycosylated and total proteins in a HepG2 (Human liver carcinoma cell line) SLC35b4 knockdown cell line. Western blot analysis, using a primary antibody against O-glycosylated proteins, showed one differentially expressed O-glycosylated protein in a HepG2 cell line knockdown of SLC35b4. Its size was estimated to be 67.5 kDa. The 2D electrophoresis study of SLC35b4 knockdown resulted in the differential expression of 10 proteins, more than 2 fold, as compared to control siRNA. Moreover, 3 of the differentially expressed proteins (corresponding to Spots SSP 6203, 6204 and 8102) have very close matches in O-glycosylated proteins of the insulin resistance pathway where O-glycosylation might play a role in glucose synthesis. The identification of the differentially expressed protein is a must in order to assess SLC35b4 role in the insulin resistance (IR) pathway using its knockdown.

Keywords: Type II diabetes, Two Dimensional electrophoresis, SLC35b4, O-glycosylated proteins

TABLE OF CONTENTS

LIST OF TABLES

LIST OF FIGURES

GLOSSARY

1D electrophoresis: One Dimensional electrophoresis

1D-SDS PAGE: One Dimensional-SDS Poly Acrylamide Gel Electrophoresis

2D electrophoresis: Two Dimensional electrophoresis

APS: Ammonium Persulfate

BARN: Blotting and Removing of Nitrocellulose

BMI: Body Mass Index

BSA: Bovine Serum Albumin

CID: Collision-Activated Dissociation

CR: Calorie Restriction

CRTC2: CREB regulated transcription coactivator 2

CSSs: Chromosome Substitution Strains

DMEM: Dulbeco's Modified Eagle Medium

FBS: Fetal Bovine Serum

GAG: glycosaminoglycan

HBP: Hexosamine Biosynthesis Pathway

HepG2: human liver carcinoma cell line

IEF: Isoelectric Focusing

IPG: Immobilized pH gradient

IR: Insulin Resistance

KD: Knockdown

MALDI TOF: Matrix-Assisted Laser-Desorption/Ionization Time-Of-Flight Mass Spectrometry

NCD: Non-Communicable Disease

O-GlcNAC: O-linked glycosylation

PBS: Phosphate Buffer Saline

PenStrep: Penicillin-Streptomycin

pI: Isoelectric Point

PMF: Peptide Mass Fingerprinting

QTLs: Quantitative Trait Loci

SDS: Sodium Dodecyl Sulfate

SNP: Single Nucleotide Polymorphism

TAE: Tris-Acetate-EDTA

TGS: Tris-Glycine-SDS

CHAPTER ONE
LITERATURE REVIEW

1.1. Type II diabetes

Diabetes is considered a Non-Communicable Disease (NCD). By definition, it may not be transmitted from one organism to another. In 2008, 57 million deaths occurred worldwide. NCDs, mainly cancer, cardiovascular diseases, diabetes, and chronic respiratory diseases were the cause of 63% (36 million) of all deaths occurring in 2008 (Alwan *et al.*, 2010). Diabetes alone caused 1.3 million deaths. As a disease, it may be categorized into 2 main branches: Type I diabetes (formerly known as insulin-dependent or juvenile diabetes) and Type II diabetes (formerly known as non-insulin dependent diabetes or adult-onset diabetes) (Shivashankar & Mani, 2011).

Glucose discharge, in the liver, is ordinarily suppressed by insulin (Melmed *et al.*, 2011). Occurring mainly within fat tissue and the liver, insulin resistance is characterized by the incapability of cells to react effectively to standard levels of insulin (Lippincott, 2007). Thus, when insulin resistance sets in, the liver unsuitably releases glucose into the blood (Melmed *et al.*, 2011). Therefore, Type II diabetes is caused by the lack of insulin production from liver beta cells in the aftermath of insulin resistance (Masharani & German, 2011). The disease pathophysiology is balanced between two conditions: either a primary insulin resistance with only a small defect in insulin secretion or a secondary insulin resistance where the primary issue would be a shortage of insulin secretion (Masharani & German, 2011).

Identified genetic variants of Type II Diabetes do not currently account for its heritability as they only justify 10% of the heritability (Billings & Florez, 2010; Wheeler & Barroso, 2011). Morbidity has been reduced radically by lifestyle modifications or medications, such as sulfonylureas or metformin, which control the resulting hyperglycemia but fail to achieve optimal glycemic levels. Hence, micro-vascular complications that are partially caused by fluctuations in glycemic levels are still an issue (Nathan *et al.*, 2009).

Type II diabetes is a genetically complex disease (Freeman & Cox, 2006). Studies of such multifactorial traits are performed on chromosome substitution strains (CSSs) of mammals to obtain congenic strains that have considerable power to detect quantitative trait loci (QTLs) reliably and reproducibly (Yazbek *et al.*, 2011). Mapping the molecular pathways and new genes involved in obesity induced type II diabetes will help in its prognosis. Using dual studies; genetic and functional, the solute receptor SLC35b4 was identified as a regulator of obesity, insulin resistance and gluconeogenesis (Yazbek *et al.*, 2011).

1.2. SLC35B4

To unravel the causal pathophysiology that in turn would offer a novel understanding of the molecular basis of the disease, the genetic factors stimulating diabetes and obesity predisposition must be identified (Altshuler *et al.*, 2008). Towards this end, Yazbek *et al.* found that Slc35b4 hepatic expression was increased ~50% in strain 6C2d-2 relative to strain 6C2d-3 ($p < 0.05$). Liver was also found to be insulin resistant in the euglycemic-hyperinsulinemic clamp experiments, as evidenced by the inability to respond to insulin and shut down glucose production. Together, this suggests that a liver autonomous defect is responsible for the hepatic insulin resistance (Yazbek *et al.*, 2011). Variation in hepatic Slc35b4 expression and altered hepatic gluconeogenesis together suggest that a liver autonomous defect is responsible for the hepatic insulin resistance. In vitro assays in human liver cell line (HepG2) also showed that a 60% alteration in Slc35b4 expression caused a 20% decrease in glucose production (Yazbek *et al.*, 2011).

Interestingly, a single nucleotide polymorphism (SNP) in the human SLC35B4 gene (rs1619682) was associated with waist circumference in the Framingham Heart Study (Fox *et al.*, 2007). The human SLC35B4 gene is located on chromosome 7q33 where QTLs have been reported that regulate body mass index (BMI), metabolic syndrome, lipid profiles, fasting glucose, pro-insulin levels, and fat stores (Arya *et al.*, 2002; Feitosa *et al.*, 2002; Tang *et al.*, 2003; Saunders *et al.*, 2007; Laramie *et al.*, 2008). Other nearby candidate genes includes LEPTIN and SEC8, and data obtained by Yazbek *et al.* indicate that SLC35B4 should be considered a strong candidate gene as well (Yazbek *et al.*, 2011). Of note, the interval spanning 7q21.1 -7q34 appears to contain at least two genes influencing obesity and obesity related traits (Li *et al.*, 2003). Further studies are needed to determine whether additional QTLs are present at this locus in humans and to establish the causal variant underlying these QTLs.

Slc35b4 encodes a protein that transports UDP-xylose and UDP-N-acetylglucosamine from the cytosol into the golgi (Ashikov *et al.*, 2005). Therefore, over-expression of Slc35b4 may alter the cellular localization of its cargo nucleotide sugars.

1.3. O-Glycosylation

UDP-xylose is required for glycosaminoglycan (GAG) biosynthesis on the core protein of proteoglycan sugar chains (Moriarity *et al.*, 2002). Proteins that are post-translationally modified with a proteoglycan function in a variety of cellular and physiological activities, including differentiation, signaling, adhesion, cell division, and wound repair (Wang *et al.*, 2007). UDP-xylose is also part of a trisaccharide found on the epidermal growth factor repeats of proteins, such as Notch and the coagulation Factors VII and IX (Hase *et al.*, 1988; Moloney *et al.*, 2000). Data from mutant Chinese hamster ovary cells that contain cytoplasmic, but not Golgi UDP-xylose synthesis demonstrated the in vivo ability of cytoplasmic UDP-xylose to be incorporated into protein xylosylation in the Golgi (Bakker *et al.*, 2009). This suggests a potential role for Slc35b4, which is the only known cytoplasmic to Golgi transporter of UDP-xylose, in the biosynthesis of GAGs and protein xylosylation.

Slc35b4 is also a transporter for UDP-N-acetylglucosamine, which is the major end product of the hexosamine biosynthesis pathway (HBP). UDP-N-acetylglucosamine then serves as both a substrate for O-linked glycosylation (O-GlcNAC) and as a negative feedback inhibitor of the HBP pathway (Buse, 2006). Alterations in the hepatic HBP flux lead to endoplasmic reticulum stress, lipid accumulation, and inflammation that could all contribute to the development of obesity and insulin resistance (IR) (Sage *et al.*, 2010). Phosphoinositide-dependent regulation of insulin signaling through O-GlcNAC modification of Akt and IRS1 represents a molecular mechanism linking the HBP pathway to IR (Yang *et al.*, 2008). In addition, the HBP pathway stimulates hepatic gluconeogenesis through an insulin-independent O-GlcNAC modification of CREB regulated transcription coactivator 2 (CRTC2) (Dentin *et al.*, 2008). Although these individual proteins are likely important to pathogenesis, over 600 proteins are modified with the addition of an O-GlcNAC moiety and may therefore contribute to the phenotype (Love & Hanover, 2005).

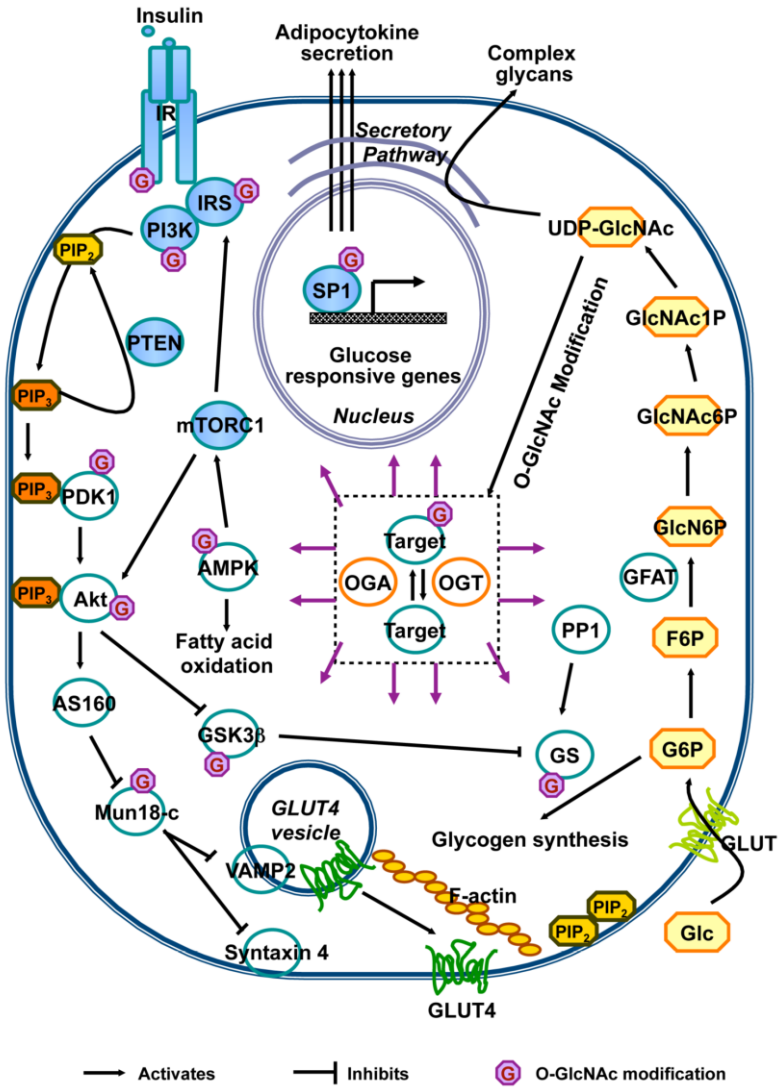

Figure 1.1. O-Glycosylated proteins in the glucose homeostasis pathway (Teo *et al.*, 2010).

Yazbek *et al.* hypothesized that hepatic over-expression of Slc35b4 alters transport and therefore bioavailability of UDP-xylose and UDP-N-acetylglucosamine (Yazbek *et al.*, 2011). Importantly, even a modest 20% increase in O-GlcNAC transferase levels leads to increased insulin resistance, suggesting that levels of UDP-N-acetylglucosamine levels are tightly regulated (McClain *et al.*, 2002). Therefore, the 1.5-fold increase in hepatic Slc35b4 mRNA levels is predicted to alter the post-translational modification of many proteins.

O-GlcNAC is exclusively located in the cytoplasm and the nucleus where it modulates the activity of several proteins and transcription factors including Sp1, CRTC2 and FoxO1 (Issad & Kuo, 2008). O-GlcNAC modification sites are often identical to or near phosphorylation sites and can therefore regulate protein function on their own or

through the inhibition of phosphorylation. The link between HSP and insulin resistance and diabetes has previously been shown to stimulate hepatic gluconeogenesis through O-GlcNAC modification of CRTC2 and FoxO1 (Lefebvre *et al.*, 2010). In addition, overexpression of UDP-N-acetylglucosamine in rat muscle causes whole body insulin resistance (Arias & Cartee, 2005).

Table 1.1. Insulin receptor pathway O-glycosylated proteins

IRS	135 kDa
PI3K	43 kDa
PDK1	49 kDa
Akt	55 kDa
Mun18-c	45 kDa
GSK3β	46 kDa
AMPK	30 kDa
SP1	83 kDa
IR	156 kDa

To this end, this study employs 1D and 2D electrophoresis to investigate differentially expressed O-glycosylated and total proteins in a HepG2 SLC35B4 knockdown cell line.

1.4. Proteomics Expression Analysis

Several protein analysis methods have been put to use in the field of proteomics, of which mass spectrometry has proved to be a proficient tool in protein and pathway identification (Marko-Vargas, 2005). Routine protein techniques like one dimensional electrophoresis and peptide mass fingerprinting, may be used to gather significant information about the glycosylation of glycoproteins (Wilson *et al.*, 2009)

1.4.1. 1D-SDS PAGE (Western Blot)

Almost four decades ago, a technique was devised for the electrophoretic transfer of proteins from polyacrylamide gels to nitrocellulose paper. Immunoblotting using specific primary and secondary antibodies was used to detect the immobilized proteins (Towbin *et al.*, 1979). As the term southern blot was already taken for the technique used to detect DNA using agarose gels, the technique was dubbed Western blotting and has become essential as a tool in the study of the presence, relative abundance, relative molecular mass, post-translational modification, and interaction of specific proteins (MacPhee, 2010).

1.4.2. 2D Electrophoresis

2D electrophoresis is a form of electrophoresis where proteins are first separated based on their isoelectric point (pI), and then separated according to their molecular weight. This allows for a far better resolution than one dimensional gel electrophoresis where proteins are only separated according to molecular weight. (Friedman *et al.*, 2009; Westermeier & Schickle, 2009). The profiling of the differentially expressed proteins can then be compared to gene expression array data available with pI from a previous experiment.

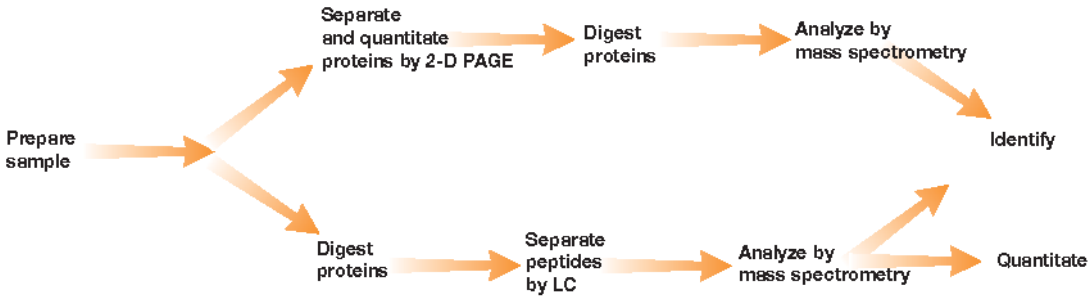

Figure 1.2. 2D Workflow suggested by Bio-Rad. Upper pathway was utilized for the purpose of this study.

Recently, Karthik *et al.* identified 4 differentially expressed proteins in a proteomic analysis of plasma proteins in diabetic rats by 2D electrophoresis, showing the value of proteomic approach in the study of the molecular basis of diabetes mellitus (Karthik *et al.*, 2012). Unpublished microarray data of Yazbek *et al.*, shows several under & over-expressed pathways, when comparing B6 and A/J mouse models.

1.4.3. MALDI Analysis

Ions from biological molecules such as proteins and DNA are produced following soft ionization as one provided by matrix-assisted laser-desorption/ionization time-of-flight mass spectrometry (MALDI TOF) (Lay & Holland, 2000). Peptide mass fingerprinting (PMF) and de novo sequencing are 2 ways through which MALDI TOF may be used to identify proteins. In PMF, a series of peptide masses are produced after proteolysis, enabling their detection by MALDI TOF and resulting in unique spectra for every protein. Databases such as SwissProt will enable the identification of most proteins after PMF (Marvin *et al.*, 2003). MALDI de novo sequencing allows sequencing of unknown

proteins one amino acid at a time through collision- activated dissociation (CID) (Seidler, 2010).

In a previous study, Hanisch was able to successfully use the MALDI TOF/TOF to localize O-glycosylation sites in glycoproteins through peptide sequencing (Hanisch, 2011).

1.5. Objectives:

- The long-term developmental objective of this research project is to apply the obtained knowledge enabling the development of novel therapeutic tools, which may lead to clinical trials and better patient treatment.

- We hope to identify, through peptide mass fingerprinting, differentially expressed O-glycosylated proteins in the insulin resistance pathway behind type II diabetes.

- The study also aims at finding and eventually identifying any differentially expressed proteins between a knockdown model of HepG2 cells and one of a control using 2D electrophoresis, hypothesizing that these proteins will be involved in the insulin resistance pathway.

CHAPTER TWO
MATERIALS AND METHODS

2.1. Cell Culture of HepG2 Cells

- Cells were maintained in Dulbeco's Modified Eagle Medium (DMEM) (Lonza) containing 10% Fetal Bovine Serum (FBS) (Sigma) and 1% Penicillin-Streptomycin (PenStrep) (Lonza)
- Cells were detached for plating by aspirating DMEM then washing with Phosphate Buffer Saline (PBS) (Sigma) after which 2 mL of 1X Trypsin (Sigma) were added for 10 minutes then deactivated by the addition of DMEM onto detached cells

2.2. Knockdown of SLC35b4

- Trilencer-27 siRNA Kit (OriGene) was used to knockdown SLC35b4 in cell culture.
  - Kit information: SLC35b4 (Human) - 3 unique 27mer siRNA duplxes – 2 nmol each (Cat # SR313733)
  - Modifications to manufacturer protocol:
    - Transfection reagent used was DharmaFECT 1 (Dharmacon)
    - Final siRNA concentration per well (in a 6well plate) was 100 nm

2.3. One-Dimensional Electrophoresis Workflow:

2.3.1. RNA Extraction

Cells from cell culture were scraped with Trizol (Invitrogen) in order to maintain RNA integrity, and then RNA was extracted using Nucleospin RNA II (Macherey-Nagel) as per manufacturer instructions. RNA integrity was checked by running 8 μL of extracted RNA in a 1.5% Agarose (Bio-Rad) gel in 1X Tris-Acetate-EDTA (TAE) buffer (Bio-Rad).

2.3.2. cDNA Synthesis

2 μL of extracted RNA was reverse transcribed into cDNA using iScript Reverse Transcription Supermix (Bio-Rad).

2.3.3. Real-Time PCR

Fluorescence Realtime PCR assay to confirm SLC35b4 knockdown was performed as follows on Roche LightCycler instrument

SLC35b4 Primers: (TIB MOLBIOL)

Forward Primer	5' - ggAggCTTTgTTTTATAATCACg
Reverse Primer	5' - AgTgATgATGTTCATgAggAggT

SLC35b4 Fluorescent Probes: (TIB MOLBIOL)

FL probe	5' - gAACTgCATggTCATAAATATCAgAAgCC-- FL
LC probe	5' - LC640-AgAAgACgAAACCCggAAgTggA-- PH

- A Primers/Probe mix for the internal control H6PD was obtained from the LightCycler h-G6PDH Housekeeping Gene Set (Roche)

The real-time PCR conditions were set as follows:

Vrxn = 20 µL

SLC35b4	**Final Conc**	**1 Reaction**
Freshly prepared Master Mix 5X LightCycler Taqman Master (Roche)	1X	4 µL
Forward Prime	300 nM	0.3 µL
Reverse Primer	300 nM	0.3 µL
Probe: SLC35B4 FL	300 nM	0.3 µL
Probe: SLC35B4 LC	300 nM	0.3 µL
Adjust volume to 15 µL with nuclease-free water		9.8 µL
	Total Volume	15 µL
Material to be quantified (Sample cDNA, water control)		5 µL

G6PDH	**Final Conc**	**1 Reaction**
Freshly prepared Master Mix 5X LightCycler Taqman Master	1X	2 µL
Primer/HybProbe Mix (detection Mix)	1X	2 µL
$MgCl_2$ stock solution (25mM)	4 mM	2.4 µL
Adjust volume to 15 µL with nuclease-free water		8.6 µL
	Total Volume	15 µL
Material to be quantified (Sample cDNA, water control)		5 µL

PCR Program:

Temperature (°C)	Time	Cycles	Acquisitions
50	2 min	X 1	None
95	10 min	X 1	None
95	10 sec	X 50	None
57	45 sec		Single
72	5 sec		None

2.3.4. Protein Extraction

Following knockdown cells were scraped in 1mL complete Laemmli buffer (Bio-Rad) and then lysed at 95^{O}C for 5 min

2.3.5. Protein Quantification

The extracted proteins were quantified using the RC DC protein quantification assay (Bio-Rad) using a Bovine Serum Albumin (BSA) (Bio-Rad) standard curve in LaemmLi Buffer (Bio-Rad)

2.3.6. One-Dimensional Gel Electrophoresis and Blotting (Western Blot)

2.3.6.1. Gel preparation:

25 mL (enough for 2 mini gels, 8 cm) of 8% (Acrylamide) SDS-PAGE lower gel was prepared as follows:

Component	Volume
H_2O	12.1 mL
4X Resolving Buffer*	6.25 mL
37.5:1 Acrylamide:Bis*	6.67 mL
10% (w/v) Ammonium Persulfate (APS)*	130 µL
TEMED*	14 µL
10% (w/v) Sodium dodecyl sulfate (SDS)*	100 µL

*Marks a product from Bio-Rad

10 mL (enough for 2 mini gels, 8 cm) of 5% (Acrylamide) SDS-PAGE upper gel was prepared as follows:

Component	Volume
H_2O	5.8 mL
4X Stacking Buffer*	2.5 mL
37.5:1 Acrylamide:Bis*	1.7 mL
10% (w/v) Ammonium Persulfate (APS)*	40 µL

TEMED*	20 μL
10% (w/v) Sodium dodecyl sulfate (SDS)*	100 μL

*Marks a product from Bio-Rad

2.3.6.2. Protein load and run parameters:

- 30-35 μL of protein volume in sample buffer was loaded in each well depending on the sample's concentration, a total of 20 μg of protein was loaded per well
- 7 μL of a 10-250 Kd protein ladder (Bio-Rad) was loaded to ensure run and transfer efficiency
- Tris-Glycine-SDS (TGS) 10X buffer (Bio-Rad) was diluted to 1X and used in electrophoresis run
- Electrophoresis run parameters were set to 100 volts until dye front reached bottom of gel

2.3.6.3. Transfer to nitrocellulose membrane:

- Transfer buffer (1 L) was prepared as follows:

Component	Volume
H_2O	800 mL
Tris (Bio-Rad)	3 g
Glycine (Bio-Rad)	14.4 g
Methanol*	200 mL

*Methanol is added to the transfer preparation tray before the H_2O (containing Tris and Glycine)

- Nitrocellulose membrane is cut at 5.5 x 8 cm
  - Soak in Methanol for 5 sec
  - Soak in H_2O for 1 min
  - Soak in transfer buffer
- Soak gel in transfer buffer for 10 min
- Transfer sandwich was prepared as follows:
  - Cassette white side down and black side up
  - Sponge, filter, membrane, gel, filter, sponge
- Place sandwich in cassette holder and cover to the rim with transfer buffer and place magnet inside. Have black side of cassette face the black side of the holder.

- Place transfer chamber on magnetic stirrer and have magnet set to slowly rotate
- Run at 110V for 1 hour

2.3.6.4. Blotting with antibodies:

- Membrane was removed and blocked with 5% non-fat milk (Regilait) in washing buffer
- Washing buffer (1L) was prepared as follows and adjust pH to 7.4 using strong acid:

Component	Volume
H_2O	1000 mL
Tris-Cl (Bio-Rad)	1.576 g
NaCl	8.77 g
Tween-20 (Bio-Rad)	0.5 mL

- Membrane was removed and blocked with 5% non-fat milk (Regilait) in washing buffer (50mL) for 2 hours
- Primary antibody was prepared in 1% non-fat milk in washing buffer at appropriate dilution
  - Membrane was incubated with 4 mL of diluted primary antibody overnight at 4°C in cold room on an orbital shaker

Primary Antibody	Dilution Factor
Monoclonal Anti-β-O-Linked *N*-Acetylglucosamine antibody (Mouse) (Sigma-Aldrich)	1:2000
Anti-Actin antibody (Rabbit) (Sigma-Aldrich)	1:4000

- Membrane was washed in washing buffer for 3X 10 min, using 25 mL of buffer each time
- Secondary antibody was prepared in 1% non-fat milk in washing buffer at appropriate dilution
  - Membrane was incubated with 4mL of diluted secondary antibody for 2 hours at room temperature on an orbital shaker

Secondary Antibody	Dilution Factor
Donkey Anti-Mouse IgG (Jackson ImmunoResearch)	1:5000
Donkey Anti-Rabbit IgG (Jackson ImmunoResearch)	1:5000

- Membrane was washed in washing buffer for 3X 10 min, using 25 mL of buffer each time
- Protein bands were visualized with the Immun-Star™ WesternC™ Chemiluminescence Kit (Bio-Rad) using the ChemiDoc™ XRS System (Bio-Rad) and the Quantity One 1-D Analysis software (Bio-Rad)

2.3.7. Matrix-Assisted Laser Desorption Ionization - Time of Flight Mass Spectrometry (MALDI-TOF MS)

- Differentially expressed band was excised from membrane blindly by using ladder and transparency print-out of captured chemiluminescence image as a guide
- Protocols followed to attempt protein identification were:
  - Use of Nitrocellulose Membranes for Protein Characterization by Matrix-Assisted Laser Desorption/Ionization Mass Spectrometry by Luque-Garcia *et al.*. (2006)
  - Analysis of Electroblotted Protein by Mass Spectrometry: Protein Identification After Western Blotting by Luque-Garcia *et al.*. (2008)

2.4. Two-Dimensional Electrophoresis Workflow:

2.4.1. RNA Extraction

Cells from cell culture were scraped with Buffer RA1 (Macherey-Nagel) in order to maintain RNA integrity, and then RNA was extracted using Nucleospin RNA II (MN) as per manufacturer instructions. RNA integrity was checked by running 8 µL of extracted RNA in a 1.5% Agarose (Bio-Rad) gel in 1X Tris-Acetate-EDTA (TAE) buffer (Bio-Rad). RNA concentration/purity was measured using Nanodrop ND-1000 (Thermo).

2.4.2. cDNA Synthesis

500 ng of extracted RNA were reverse transcribed into cDNA using iScript Reverse Transcription Supermix (Bio-Rad)

2.4.3. SYBR Green Real-Time PCR

SYBR green Real-time PCR assay to confirm SLC35b4 knockdown was performed as follows on the Bio-Rad CFX96 touch instrument

- Primers were designed using the SciTools Real-time PCR tool of the Integrated DNA technologies homepage

  SLC35b4 Primers (refseq NM_032826): (TIB MOLBIOL)

Forward Primer	AAAGCAGGTGACTTCCCAG
Reverse Primer	AATATCCCCATCCTTGCTGAC

  H6PD Primers (refseq NM_004285): (TIB MOLBIOL)

Forward Primer	TGTCCTTGAGAAACCCTTTGG
Reverse Primer	GTCTCGGAAAGGCAGGATC

  *All primers were reconstituted in 650 µL of nuclease-free water in order to attain a concentration of 20 uM

- The real-time PCR conditions were set as follows:

Vrxn = 20 µL

SLC35b4	**Final Conc**	**1 Reaction**
iQ SYBR green supermix (2X)	1X	10 µL
Forward Primer	300 nM	0.3 µL
Reverse Primer	300 nM	0.3 µL
Adjust volume to 17 µL with nuclease-free water		6.4 µL
	Total Volume	17 µL
Material to be quantified (Sample cDNA, water control)		3 µL

H6PD	**Final Conc**	**1 Reaction**
iQ SYBR green supermix (2X)	1X	10 µL
Forward Primer	300 nM	0.3 µL
Reverse Primer	300 nM	0.3 µL
Adjust volume to 17 µL with nuclease-free water		6.4 µL
	Total Volume	17 µL
Material to be quantified (Sample cDNA, water control)		3 µL

PCR Program:

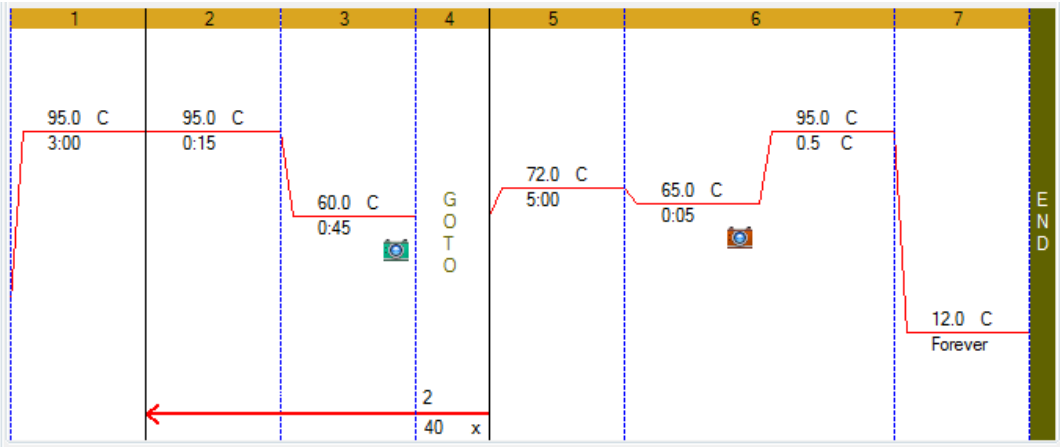

1	95.0 C for 3:00	
2	95.0 C for 0:15	
3	60.0 C for 0:45	
	+ Plate Read	
4	GOTO 2 , 40 more times	
5	72.0 C for 5:00	
6	Melt Curve 65.0 to 95.0 C, increment 0.5 C,	
	for 0:05 + Plate Read	
7	12.0 C Forever	
	END	

- A serial dilution standard curve, both for SLC35b4 and H6PD, was run parallel to samples and the Real-time PCR report was generated by the CFX manager software.

2.4.4. Protein Extraction

Following knockdown cells were scraped in 1mL 2D sample buffer (Bio-Rad) and then proteins were extracted using the ReadyPrep Total Protein Extraction Kit (Bio-Rad) according to manufacturer's instructions

2.4.5. Protein Quantification

The extracted proteins were quantified using the RC DC protein quantification assay (Bio-Rad) using a Bovine Serum Albumin (BSA) (Bio-Rad) standard curve in 2D sample buffer (Bio-Rad) following the manufacturer's instruction, including:

- Two washes were performed using the RC reagents
- Protein pellet was dried under vacuum centrifugation for 40min before proceeding to adding DC reagents

2.4.6. Protein Cleanup

The extracted proteins were cleaned using the ReadyPrep 2D cleanup kit (Bio-Rad) following the manufacturer's instructions

2.4.7. Two-Dimensional Gel Electrophoresis

2.4.7.1. Sample rehydration

- 400 μg of cleaned protein in 300 μL of 2D sample buffer were placed in a 17 cm tray and 17 cm pH 3-10 ReadyStrip IPG strips were placed gel-side down over sample buffer and covered with 3mL mineral oil (Bio-Rad) and left to rehydrate overnight (12 hours)

2.4.7.2. Isoelectric focusing (IEF)

- IEF was performed on PROTEAN® i12™ IEF System (Bio-Rad)
- Strips were drained from oil then transferred to IEF focusing tray gel-side up
- Wetted electrode wicks were placed at the ends of strip
- Electrodes were then installed in their place at tray ends

- Strips were overlaid with 7mL of mineral oil
- Focusing conditions were as follows:

Start voltage	End voltage	Volt-hours	Ramp	Temperature
0 V	10,000 V	40,000 V-hr	Rapid	20°C

2.4.7.3. SDS-Polyacrylamide gel electrophoresis (SDS-PAGE)

- 40 mL (enough for 1 XL gel) of 10% (Acrylamide) SDS-PAGE upper gel was prepared as follows:

Component	Volume
H_2O	16.8 mL
4X Resolving Buffer*	10 mL
37.5:1 Acrylamide:Bis (30%)*	13.36 mL
10% (w/v) APS*	210 μL
TEMED*	23 μL
10% (w/v) SDS*	160 μL

*Marks a product from Bio-Rad

- Prior to addition of TEMED and APS to gel solution. The solution was degased for 3min then APS and TEMED were added and solution swirled gently
- Gel solution was poured between glass plates then IPG comb (containing well for ladder) was placed (gels need around 40 min to solidify)
- Prior to placing IPG strips on gel plates, IPG comb was removed and IPG well was washed with 1X TGS buffer
- Preparation of Equilibration buffer:
  - 6 M Urea, 0.375 M Tris-HCl (pH 8.8), 2% w/v SDS, 20%v/v glycerol
- Drain strips from oil and transfer them to a new tray
- Add 5 mL Equilibration buffer I: Equilibration buffer + 2% w/v DTT (Bio-Rad) and place tray on orbital shaker for 10min
- Melt overlay Agarose (Bio-Rad) in microwave for 30 sec then leave to cool in room temperature
- Discard Equilibration buffer 1 and add Equilibration buffer II: Equilibration buffer + 2.5% w/v Iodoacetamide (Bio-Rad) and place tray on orbital shaker for 10 min

- Discard Equilibration buffer II and fill 100 mL graduated cylinder with 1X TGS buffer
- Dip IPG strips in 1X TGS buffer 5-6 times in order to get rid of excess equilibration buffer
- Lay the strip gel-side up on back plate of the gel
- Cut off the plastic edges off the IPG strip
- Place overlay agarose into IPG well and gently ease IPG strip through agarose downward until it comes to contact with gel below
- Stand gels vertically and allow agarose to solidify for 5 min prior to mounting them in the electrophoresis cell
- Fill upper and lower reservoir chambers with 1X TGS buffers
- Run conditions were set as 16 mA/gel for 30 min, 24 mA/gel for 5 hours

2.4.7.4. Staining

- Fill staining tray with distilled water
- After the SDS-PAGE run has ended, the gel cassette was opened and placed in the tray on a rocker
- The gel was washed 3 times for 5 min each, adding fresh distilled water for each wash
- Add BioSafe Coomassie stain (Bio-Rad) and stain the gel for 60 min
- Discard the stain and wash twice for 15 min each with distilled water

2.4.7.5. Imaging

- The gel was scanned using Bio-Rad's GS-800 calibrated imaging densitometer and image was aquired using the Quantity One software (Bio-Rad)

2.4.7.6. Analysis

- Analysis of differentially expressed proteins was performed using PDQuest software (Bio-Rad)

CHAPTER THREE
RESULTS

3.1. One-Dimensional Electrophoresis Workflow:

3.1.1. RNA Extraction

RNA integrity was confirmed since bands for mRNA, rRNA and tRNA were visible and no smear was observed (Figure 3.1).

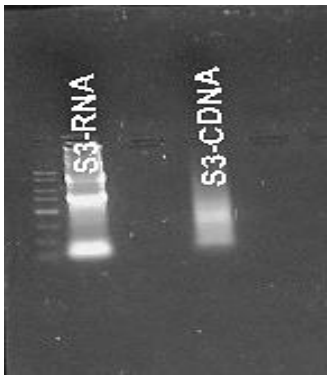

Fig. 3.1. 1.5% Agarose gel showing extracted RNA and transcribed cDNA. Bands for tRNA, mRNA and rRNA are visible without streaking thus validating RNA use for Real-Time PCR.

3.1.2. Real-Time PCR

Fluorescence Real-time PCR assay was performed on the transcribed cDNA to confirm SLC35b4 knockdown (KD) in the HepG2 cells (Figure 3.2), using G6PDH (H6PD) gene as a reference gene (Figure 3.3).

Two samples of both KD (KD1 & KD2) and control (CTL2 & CTL3) were run in duplicates and all sample curves overlap. Positive control (human) from RNA extracted and reverse transcribed and gave a positive result. Negative control showed (Ct = 37.05) and may be attributed to primer dimers.

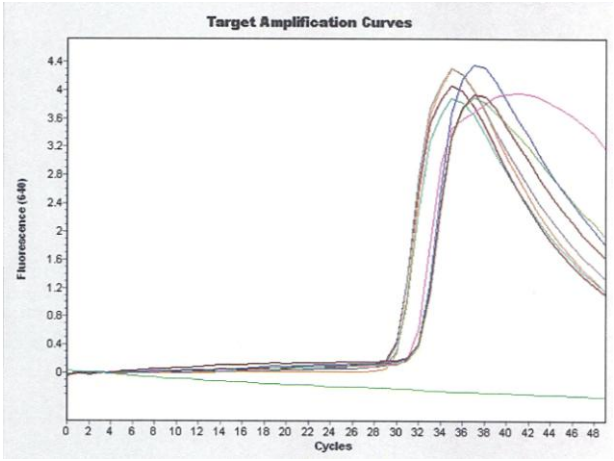

Fig. 3.2. SLC35b4 KD real-time PCR amplification curves using Roch LightCycler 2.0. Two amplification curves are noticeable: to the left are the amplification curves for the 2 control samples run in duplicates and the right are the amplifications curves for the 2 knockdown samples run in duplicates.

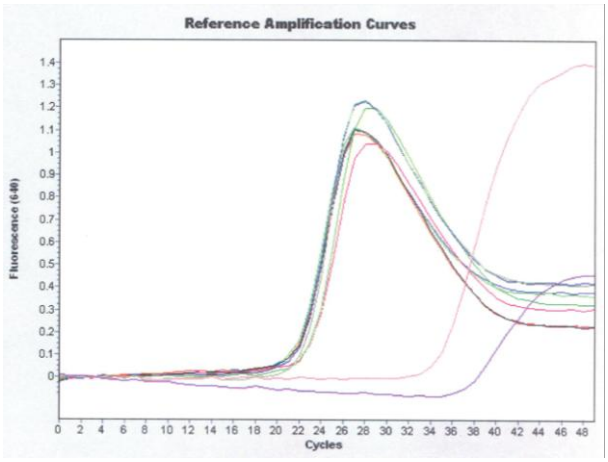

Fig. 3.3. G6PDH real-time PCR amplification curves using Roch LightCycler 2.0. One main amplification curves is noticeable: starting around 22 cycles are all amplification curves for both control and knockdown samples for the H6PD reference gene. One control sample and a negative sample are to the right.

Knockdown of SLC35b4, using H6PD as a reference gene, was calculated using the ΔCq method as shown in Table 3.1. Efficiencies of both reactions were assumed to be 100%. Final expression of SLC5b4 is calculated by dividing final averages, yielding an expression of 0.42 as compared to an expression of 1 for the H6PD reference. This indicates a 58% knockdown of the SLC35b4 mRNA in the samples.

Table 3.1. ΔCq calculations of SLC35b4 expression with respect to H6PD. Final relative expression is calculated by dividing KD averages by Ctrl averages to obtain a decrease of 58% in expression of SLC35b4 between KD and control samples

	G6PDH Ct	G6PDH Average	SLC35b4 KD Ct	SLC35b4 KD Average	Cycle Difference	Normalized by reference gene	Average
Ctrl 2	21.2	21.16	28.96	28.975	-7.775	0.004565536	0.005006877
	21.12		28.99				
Ctrl 3	21.3	21.37	28.81	28.82	-7.52	0.005448217	
	21.44		28.83				
KD 1	22.17	22.19	30.31	30.63	-8.46	0.00283979	0.002147277
	22.21		30.95				
KD 2	21.54	21.595	30.97	30.965	-9.425	0.001454763	
	21.65		30.96				

Relative expression of SLC35b4 in knockdown samples as calculated by the ΔCq method indicated a 58% decrease in expression with respect to H6PD (Figure 3.4).

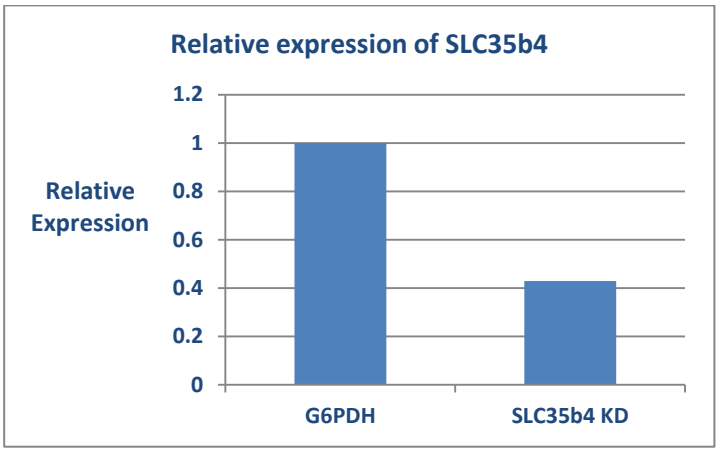

Fig. 3.4. Bar graph showing relative expression of SLC35b4 with respect to H6PD.

3.1.3. Protein Quantification

After confirmation of knockdown of SLC35b4 gene, proteins were extracted from the KD and control (Ctrl) HepG2 cells, and their concentration was determined using Bovine Serum Albumin for the standard curve (Table 3.2, Figure 3.5 & Table 3.3).

Table 3.2. Absorbance values obtained for BSA standard curve.

BSA Standard Curve			
Concentration (mg/mL)	**Absorbance 1 (λ = 750 nm)**	**Absorbance 2 (λ = 750 nm)**	**Absorbance Average**
1.5	0.8633	0.89	0.877
0.75	0.771	0.75	0.761
0.375	0.7	0.716	0.708
0.18	0.691	0.656	0.674

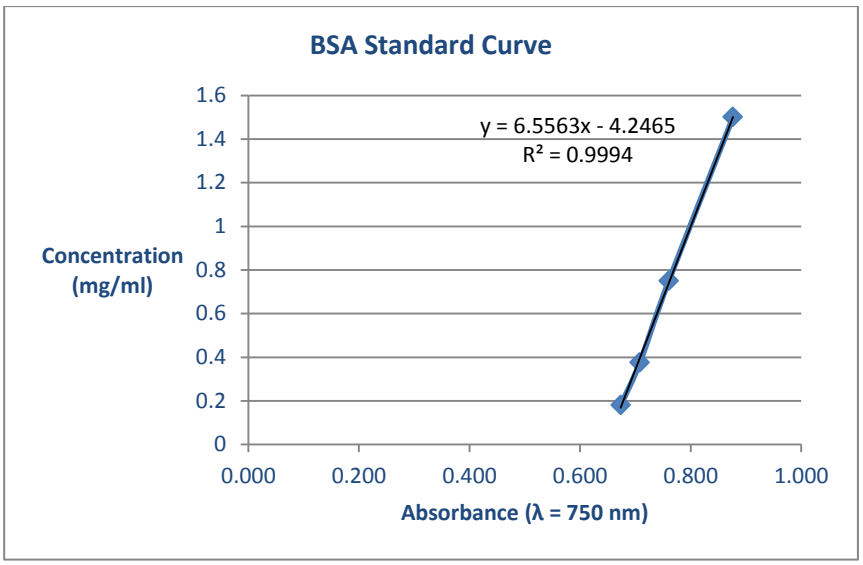

Fig. 3.5. Graph for BSA standard curve along with the best-fit linear trendline and R value.

Concentration of samples were calculated by replacing their corresponding absorbance values in the formula, y = 6.5563x - 4.2465, in place of the unknown "x". Results are shown in Table 3.3.

Table. 3.3. Absorbance values obtained for KD and Ctrl samples and their corresponding concentration from the standard curve trendline formula.

Samples				
Sample	**Absorbance 1 (λ = 750 nm)**	**Absorbance 2 (λ = 750 nm)**	**Absorbance Average**	**Concentration (mg/mL)**
KD 1	0.713	0.853	0.783	0.887
KD 2	0.721	0.874	0.798	0.982
Ctrl 2	0.845	0.84	0.843	1.277
Ctrl 3	0.829	0.895	0.862	1.405

3.1.4. One-Dimensional Gel Electrophoresis and Blotting (Western Blot)

The extracted proteins were run on 1D gel and blotted using a primary antibody against O-glycosylated proteins (Figure 3.6 & Figure 3.7). Equal loading was ensured by loading 20 μg of protein per well and placing 2 overlapping membranes during transfer the second of which was blotted using Actin primary antibody. Captured membrane image as shown in Figure 3.6 (40 seconds exposure time) reveals 7 distinct bands corresponding to O-glycosylated proteins.

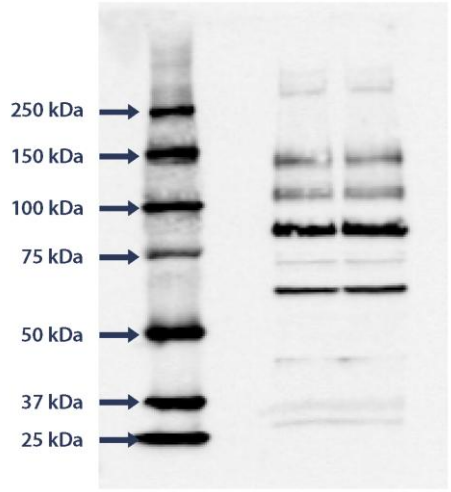

Fig. 3.6. Western blot of O-glycosylated proteins in HepG2 cell line. Seven bands corresponding for O-glycosylated proteins are noticed.

One differentially expressed protein is apparent as shown in Figure 3.7 between KD sample and control siRNA. Band is between 50-70kDa as indicated by ladder. Actin loading control, from second membrane blotted by Actin primary antibody, shows that loading was equal.

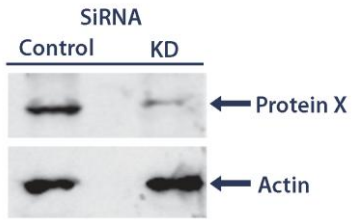

Fig. 3.7. Western blot showing difference in expression between KD and control of SLC35b4 using Actin as a loading control. A 65% reduction in protein X in noticeable.

Plotting the log of the protein size (kDa) of the ladder versus the distance they travelled (cm) (Figure 3.8), a linear trend is apparent and may be used to calculate the size of protein "X".

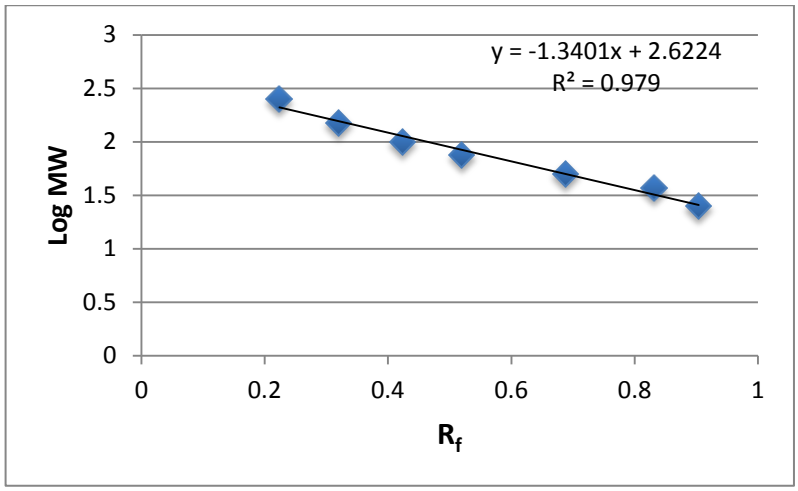

Figure 3.8. 1D standard curve of log of protein molecular weight (MW) vs. Ratio of Fronts (R_f)

3.1.5. Matrix-Assisted Laser Desorption Ionization - Time of Flight (MALDI-TOF)

- Trials to identify differentially expressed bands were conducted as per authors' instructions as mentioned in section 2.4.7 in Materials and Methods.
- Attempts were made to both strip membrane from proteins and extract proteins from it without stripping
- All resulting spot spectra showed 40-45% noise intensity and protein identification was not possible

3.2. Two-Dimensional Electrophoresis Workflow:

3.2.1. RNA Extraction

RNA integrity was confirmed since bands for mRNA, rRNA and tRNA were visible and no smear was observed (Figure 3.9).

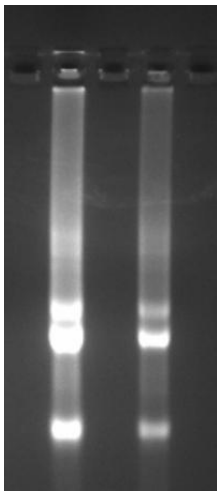

Fig. 3.9. 1.5% Agarose gel showing extracted RNA and transcribed cDNA. Bands for tRNA, mRNA and rRNA are visible without streaking thus validating RNA use for Real-Time PCR.

RNA concentration was checked using the Nanodrop in order to ensure equal amount of RNA is reverse transcribed (Table 3.4). Also 260/280 ratios were obtained in order to ensure RNA purity and absence of protein contamination. All values were close to 2 ensuring that samples may be used in reverse transcription.

Table 3.4. Absorbance values of extracted RNA as measured using Nanodrop.

Sample	Concentration (ng/µL)	Absorbance ratio 260/280
KD RNA 1	263.1	2.13
KD RNA 2	192.5	2.15
Ctrl RNA 1	551.1	2.09
Ctrl RNA 2	270	2.07

3.2.2. SYBR Green Real-Time PCR

Standard curve results of SLC35b4 serial dilution show an efficiency of 99.8% and a perfect linear fit. Samples were diluted 1/10 each time. Standard curve samples were run in triplicates and outliers were excluded from graph (Figure 3.10).

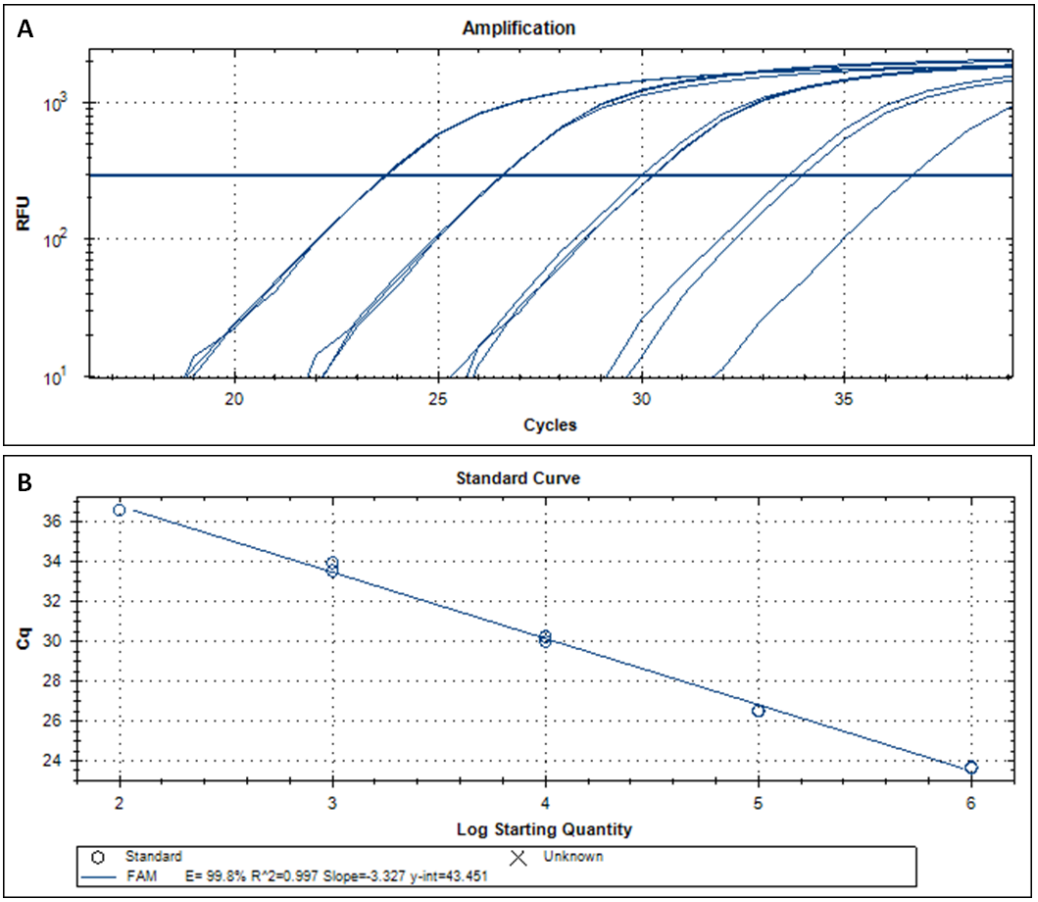

Fig. 3.10. Standard curve results of SLC35b4 dilution series. Five dilutions of DNA, each 1/10 from the previous, were performed and the standard curve generated. An efficiency of 99.8% was obtained.

Standard curve results of H6PD serial dilution (Figure 3.11) show an efficiency of 95.5% and a perfect linear fit. Samples were diluted 1/10 each time. Standard curve samples were run in triplicates and last 2 serial dilutions were excluded from graph because their quantity was too thinned out and did not exhibit any real-time amplification.

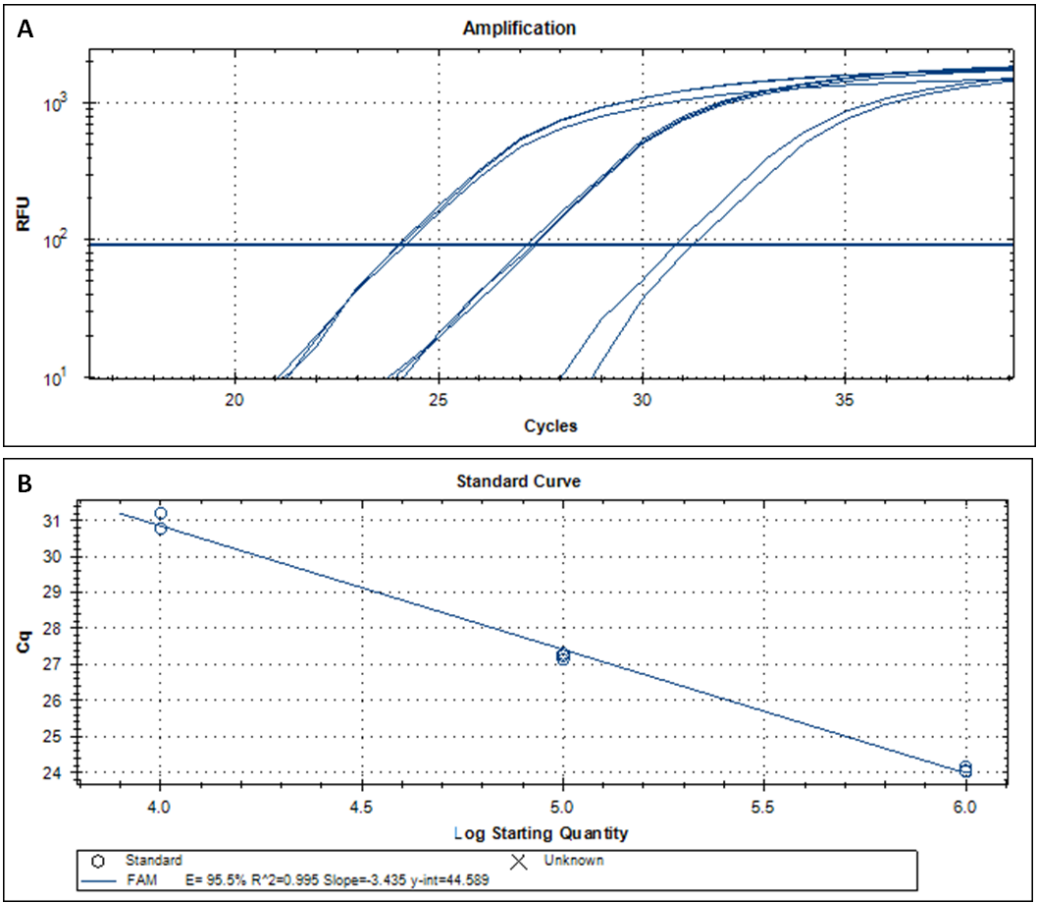

Fig. 3.11. Standard curve results of H6PD dilution series. Five dilutions of DNA, each 1/10 from the previous, were performed and the standard curve generated. An efficiency of 95.5% was obtained.

Amplification curve results of knockdown and control samples were run in duplicates. All duplicates gave very similar Cq values and were statistically valid. Negative control samples for both SLC35b4 KD and control generated a curve at a Cq > 35 which may be attributed to primer dimers (Figure 3.12).

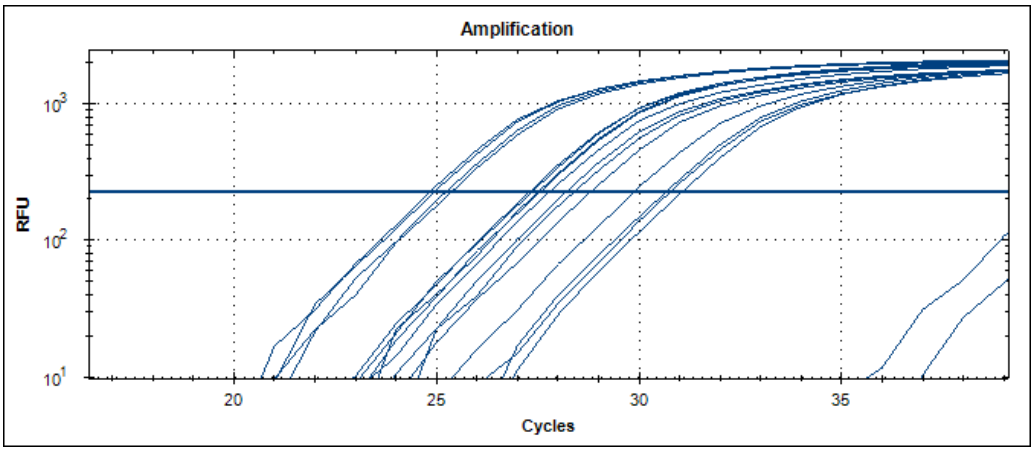

Fig. 3.12. Amplification curves of knockdown and control samples both for SLC35b4 and H6PD. Negative control samples to the right display what seem to be primer dimers.

Melt curve and melt peak results of knockdown and control samples were generated. Two melt peaks were observed (Figure 3.13), one corresponding for SLC35b4 at 81.5° C and another for H6PD at 85.5° C, indicating that no other product's amplification except these two was recorded. All SLC35b4 melt peaks were perfectly overlaid, as well as all melt peaks corresponding to samples from H6PD amplifications. Primer dimers, as previously mentioned, were also observed at 75° C to the left.

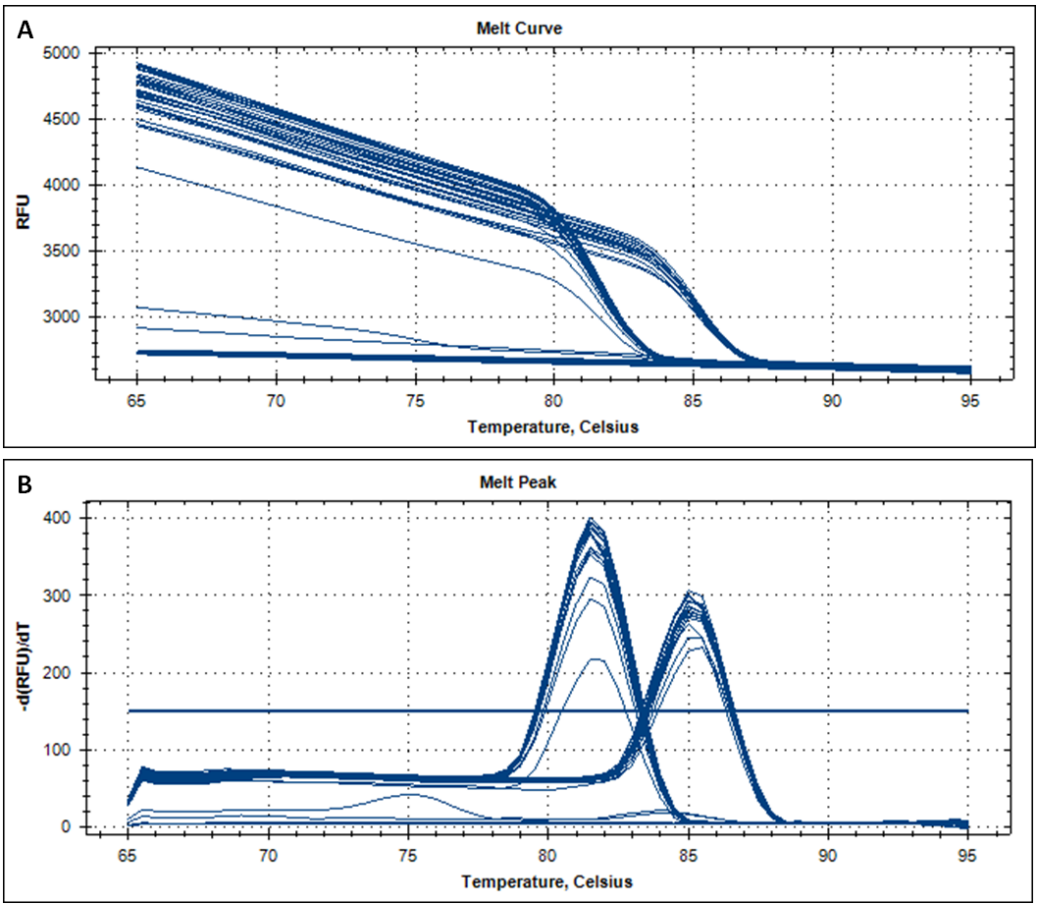

Fig. 3.13. Melt curve and melt peak analysis of both SLC35b4 and H6PD. Two peaks corresponding for H6PD and SLC35b4 are noticeable. Negative control samples display insignificant amplification.

Normalized gene expression (Figure 3.14) was calculated using the ΔΔCq method by the CFX Manager software. Results indicate no significant change of gene expression for KD 1 with respect to Control 1, and no significant change of gene expression of KD 2 with respect to Control 2. High error bars were observed in Control 1 normalized expression.

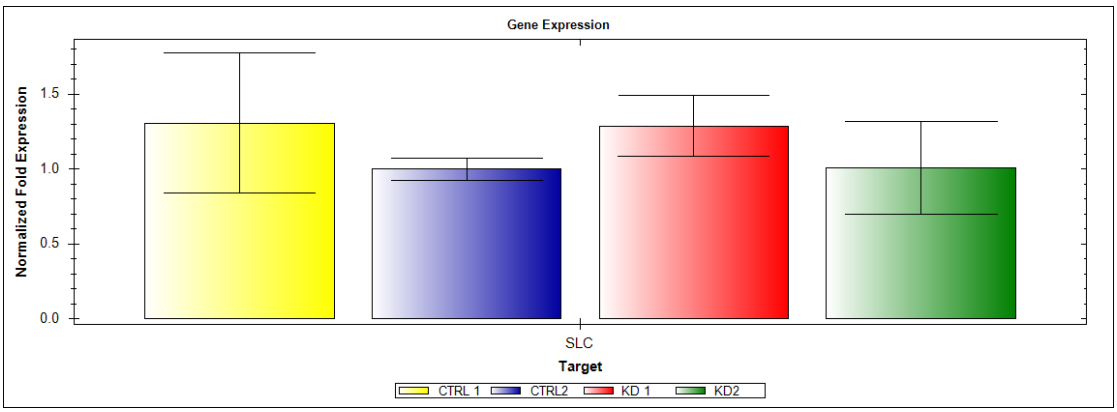

Fig. 3.14. SLC35b4 gene expression, using H6PD as a reference gene, as calculated using the ΔΔCq method by the CFX Manager software. Calculations do not show significant relative expression difference between knockdown and control samples for SLC35b4.

3.2.3. Protein Quantification

Proteins were extracted from the KD and control HepG2 cells, and their concentration was determined using Bovine Serum Albumin for the standard curve (Table 3.5, Fig. 3.15 & Table 3.6).

Table 3.5. Absorbance values obtained for BSA standard curve.

BSA Standard Curve			
Concentration (mg/mL)	**Absorbance 1 (λ = 750 nm)**	**Absorbance 2 (λ = 750 nm)**	**Absorbance Average**
3	0.494	0.465	0.480
1.5	0.316	0.326	0.321
0.75	0.235	0.231	0.233
0.375	0.185	0.21	0.198
0.18	0.183	0.177	0.180

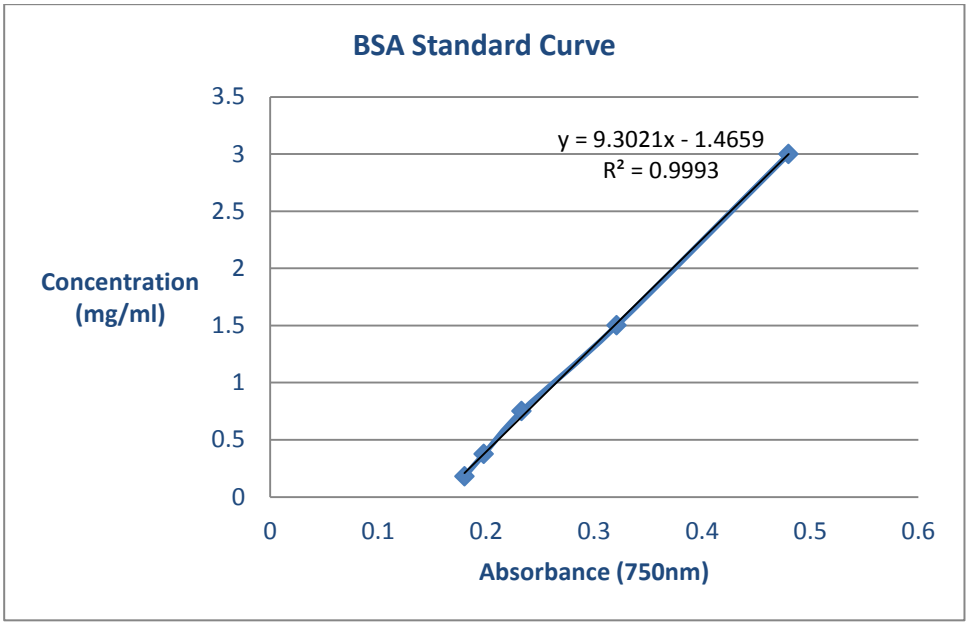

Fig. 3.15. Graph showing absorbance values obtained for BSA standard curve along with the best fit linear trendline and R value.

Concentration of samples were calculated by replacing their corresponding absorbance values in the formula, y = 9.3021x - 1.4659, in place of the unknown "x". Results are shown in Table 3.6.

Table 3.6. Absorbance values obtained for KD and Ctrl samples and their corresponding concentration from the standard curve trendline formula.

Samples				
Sample	**Absorbance 1 (λ = 750 nm)**	**Absorbance 2 (λ = 750 nm)**	**Absorbance Average**	**Concentration (mg/mL)**
KD 1	0.355	0.365	0.360	1.883
KD 3	0.372	0.378	0.375	2.022
Ctrl 1	0.473	0.447	0.460	2.813
Ctrl 3	0.551	0.548	0.550	3.646

3.2.4. One-Dimensional Gel Electrophoresis

Protein extraction using a standard 1D Laemmli buffer and using the Bio-Rad total protein extraction kit was compared to evaluate protein extraction method. Both extraction methods used yielded clean 1D gels (Figure 3.16). The extraction kit yielded a higher number of protein bands in the high molecular weight as compared to the standard extraction using Laemmli buffer, and resulted in similar protein bands in the low molecular weight proteins.

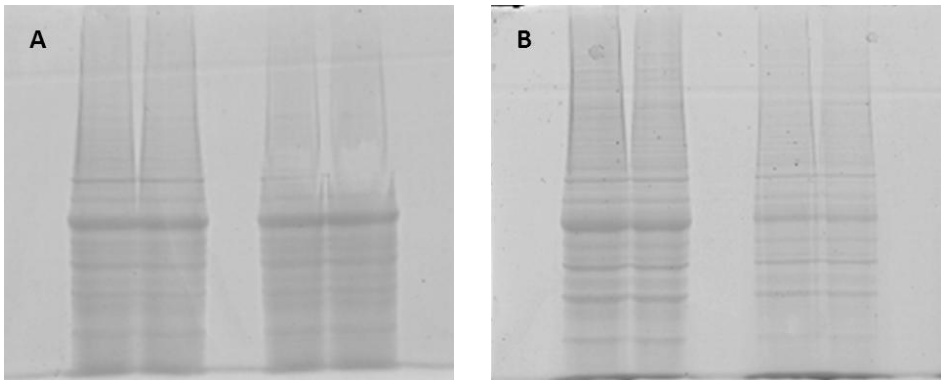

Fig. 3.16. 8% SDS-PAGE gel using HepG2 proteins extracted using (A) Laemmli buffer and heated for 3min at 95^{o} C, (B) Bio-Rad's Total protein extraction kit. Extraction kit proves more efficient than standard Laemmli buffer extraction as it shows more protein bands in the high molecular weight.

3.2.5. Two-Dimensional Gel Electrophoresis

3.2.5.1. Imaging

Total proteins extracted from HepG2 cell lines were subjected to IEF on 17cm IPG strips pH 3-10 and ran on 8% SDS-PAGE gels without (Gel A, Figure 3.17) and with cleaning (Gel B, Figure 3.17) the protein sample prior to IEF strip rehydration. Better protein resolution and spot separation, as well as a decrease in vertical streaking, was attained with cleanup and thus it was decided that KD and control samples will be cleaned prior to IEF.

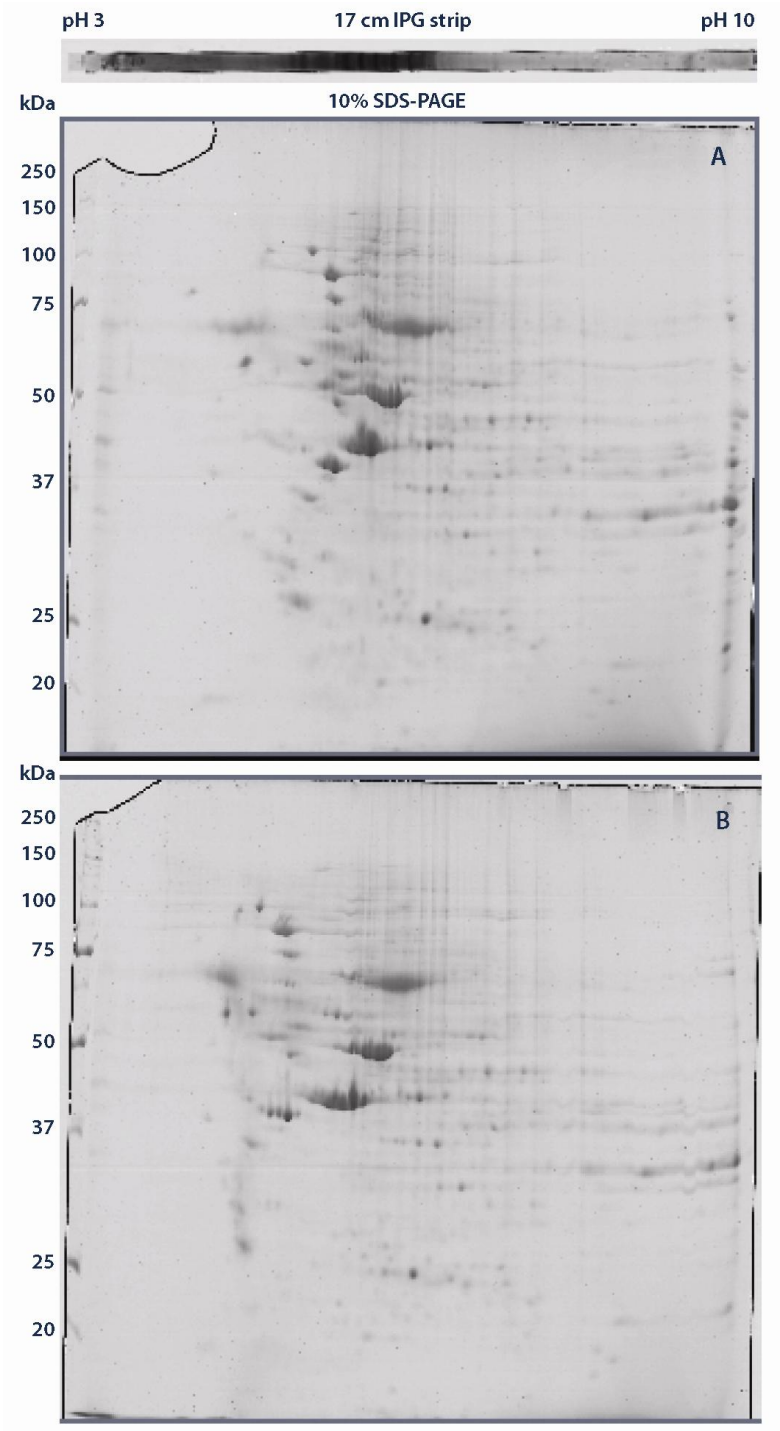

Fig. 3.17. Enhancement of protein spot separation and resolution using cleanup kit after total protein extraction. Gel (bottom) run after total protein extract was cleaned using Bio-Rad Clean-up Kit shows better spot separation and less vertical streaking.

Total proteins extracted (400 µg) from 3 KD and 3 Control samples were cleaned. IEF was performed on 17cm IPG strips ph 3-10 and ran on 10% 2D gels. One KD and control sample were excluded from the analysis because gels were not adequate. Two KD samples and 2 control samples were used to create a "Master Gel" (Figure 3.18), which overlays all existing gels for comparison purposes using the PDQuest software. Two protein clusters appear to be differentially expressed to the naked eye.

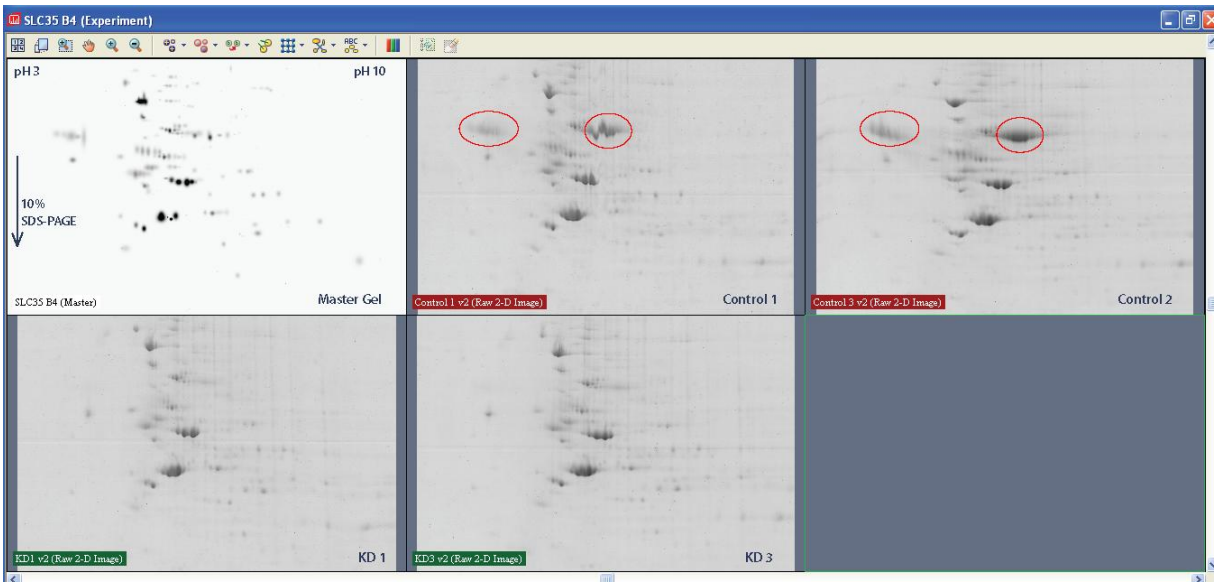

Fig. 3.18. 2D Master gel, Control gels and KD gels. PDQuest software combines all gels into one "Master Gel" which is used as a reference. Visually, 2 proteins (circled in red) are noticed to be differentially expressed (Under-expressed) between control (up) and knockdown (below) gels where they are absent.

3.2.5.2. Analysis

The selection criteria for differential expression analysis was selected to be all proteins differentially expressed (over-expressed or under-expressed) more than 2 times within a 90% confidence interval using the students' t-test. False positives, due to vertical or horizontal streaks, were then omitted from analysis. Ten differentially expressed proteins were observed (Figure 3.19), 7 of which were under-expressed with respect to control gels, and 3 of which were over-expressed. Figure 3.19 shows the proteins respective distribution on the gels.

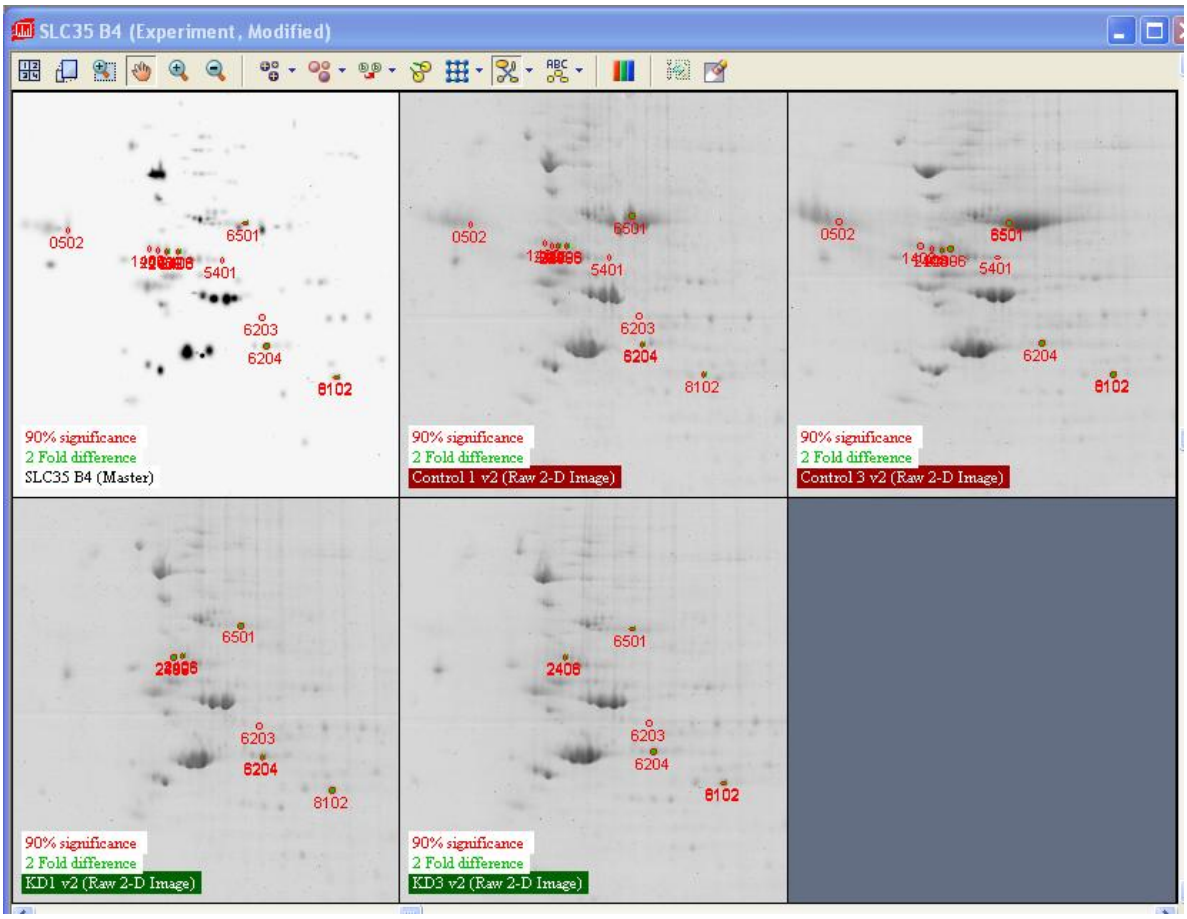

Fig. 3.19. Localization of the differentially expressed proteins on the 2D gels. After filtering though selection criteria of 2 fold difference and a 90% significance levels, 10 differentially expressed proteins may be noticed between control (up) and knockdown samples (down). This figure shows the location of those proteins on all gels including the master gel.

Table 3.7 shows the differentially expressed spots where 3 over-expressed proteins are highlighted in "Green" color and 7 under-expressed proteins are highlighted in "Purple" color. Values indicated in table are intensity values of spots as given by software following gel scan and analysis. Blank values are where software indicates a total absence of intensity. Some spots indicated by software were slightly shifted to the left or right causing a false reading of intensity.

Table 3.7. List of differentially expressed spots between knockdown and control of SLC35b4.

SSP	Control 1	Control 3	KD1	KD3
502	60	103		
1402	29.3	39.6		
2408	41.8	66.3		
5401	9.4	11.7		
6203	1		10.6	7.7
2406	52.8	66.3	12.2	20.8
2409	41	30.5	0.2	
6204	11.6	18.7	34.1	35
6501	303.6	310.9	10.7	28.6
8102	0.6	11.3	41.5	35.6

Spot SSP 2406 was localized correctly in all 4 gels and is under-expressed by 3.6 times as compared to the control gel (Figure 3.20). Manually averaging intensities of control gels and dividing by averaged intensities of KD gels determined relative expression.

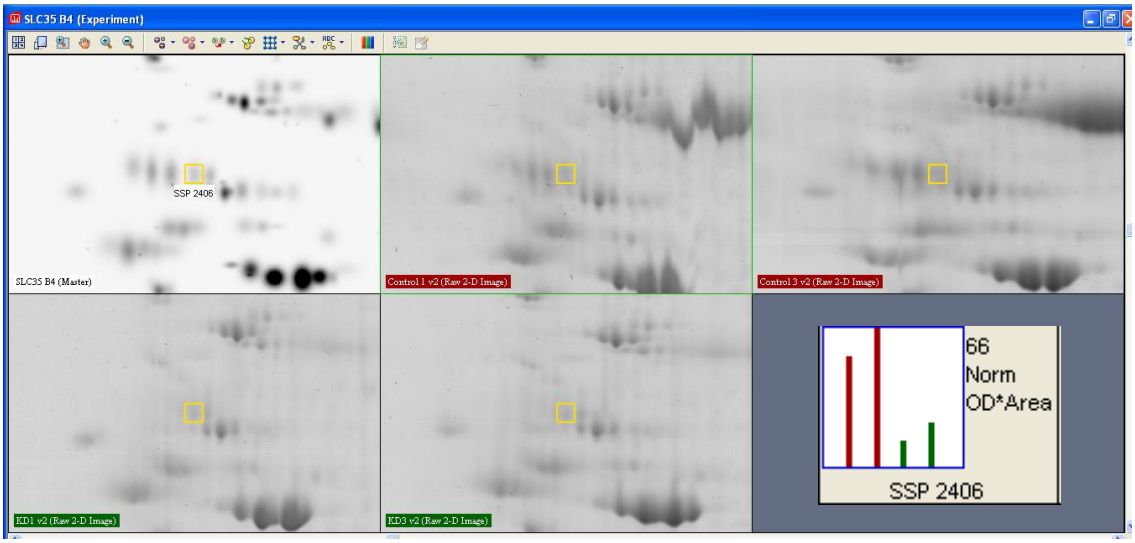

Fig. 3.20. Spot SSP 2406. Protein is under-expressed by 3.6 when comparing and averaging absorbance values for control gels as compared to knockdown gels of SLC35b4.

Spot SSP 2409 was localized correctly in all 4 gels and is completely under-expressed as intensity values from KD gels are negligible leading to the conclusion that protein expression was totally inhibited (Figure 3.21).

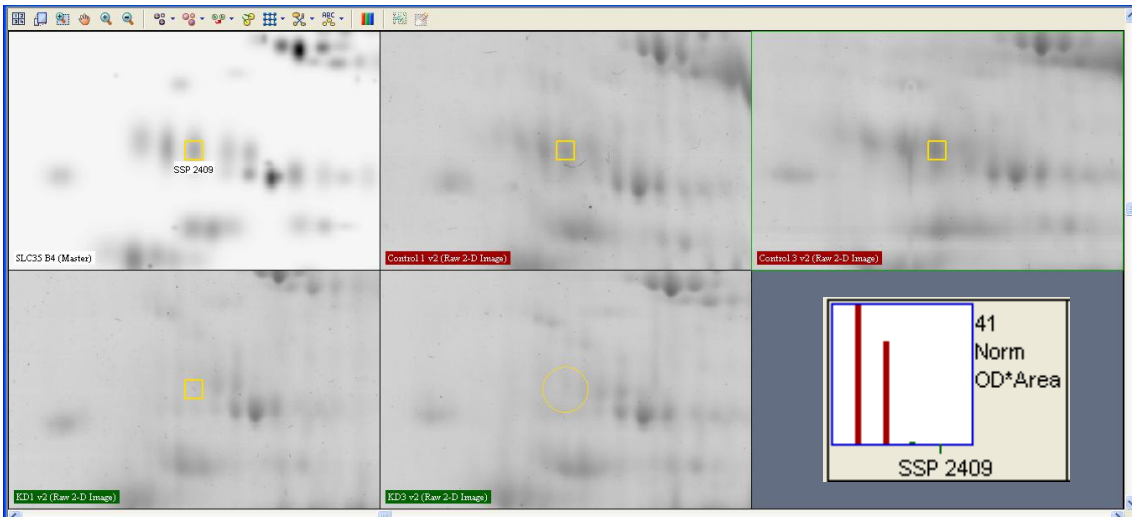

Fig. 3.21. Spot SSP 2409. Protein is completely under-expressed when comparing and averaging absorbance values for control gels as compared to knockdown gels of SLC35b4.

Spot SSP 6204 was localized correctly in all 4 gels (although it should be noted that its localization in Control Gel 1 v2 is slightly shifted to the left, but that this did not affect analysis) and is over-expressed by 2.28 times as compared to the control gel (Figure 3.22).

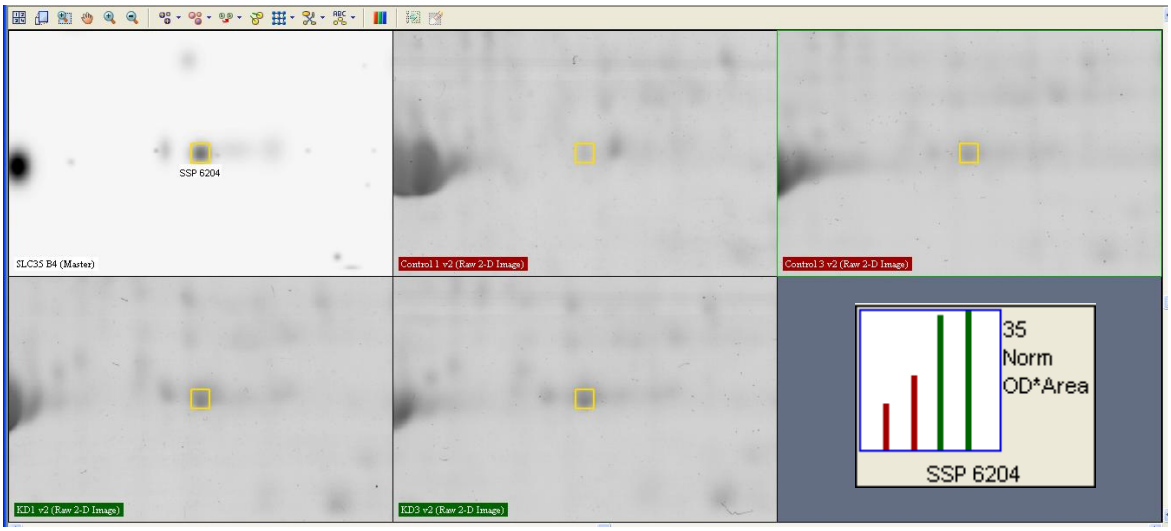

Fig. 3.22. Spot SSP 6204. Protein is over-expressed by 2.28 when comparing and averaging absorbance values for control gels as compared to knockdown gels of SLC35b4.

Spot SSP 6501 was localized correctly in all 4 gels (although it should be noted that it seemed more of a protein cluster (Figure 3.23). It was hard to determine whether it was several protein isoforms that were adjacent to each other or a single protein found in a high quantity that caused a horizontal smear) and is under-expressed by 15.6 times as compared to the control gel.

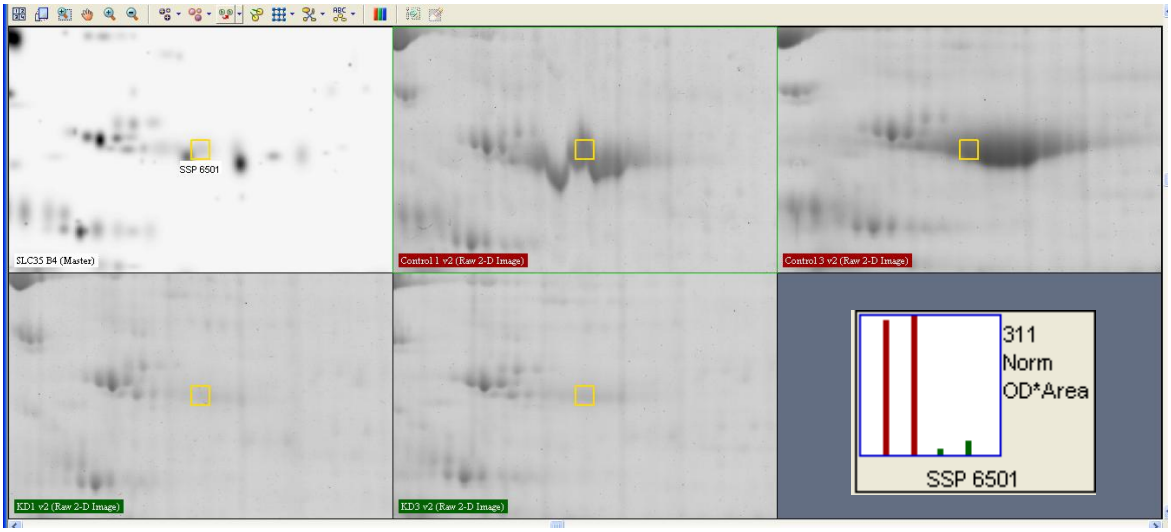

Fig. 3.23. Spot SSP 6501. Protein is under-expressed by 15 .6 when comparing and averaging absorbance values for control gels as compared to knockdown gels of SLC35b4.

SSP 8102 was localized correctly in all 4 gels (although it should be noted that its localization in Control Gel 1 v2 is slightly shifted to the left, but that this did not affect analysis) and is over-expressed by 6.42 times as compared to the control gel (Figure 3.24).

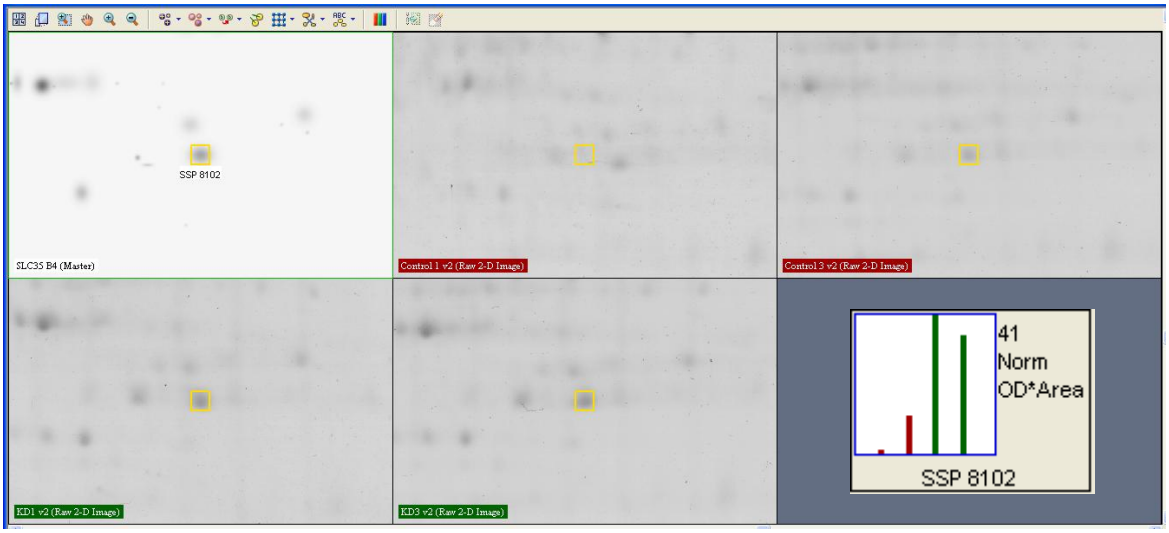

Fig. 3.24. Spot SSP 8102. Protein is over-expressed by 6.42 when comparing and averaging absorbance values for control gels as compared to knockdown gels of SLC35b4.

Spot SSP 0502 was localized correctly in all 4 gels (although it should be noted that it is part of a protein cluster that was under-expressed) and is completely under-expressed as intensity values from KD gels are negligible leading to the conclusion that protein expression was totally inhibited (Figure 3.25).

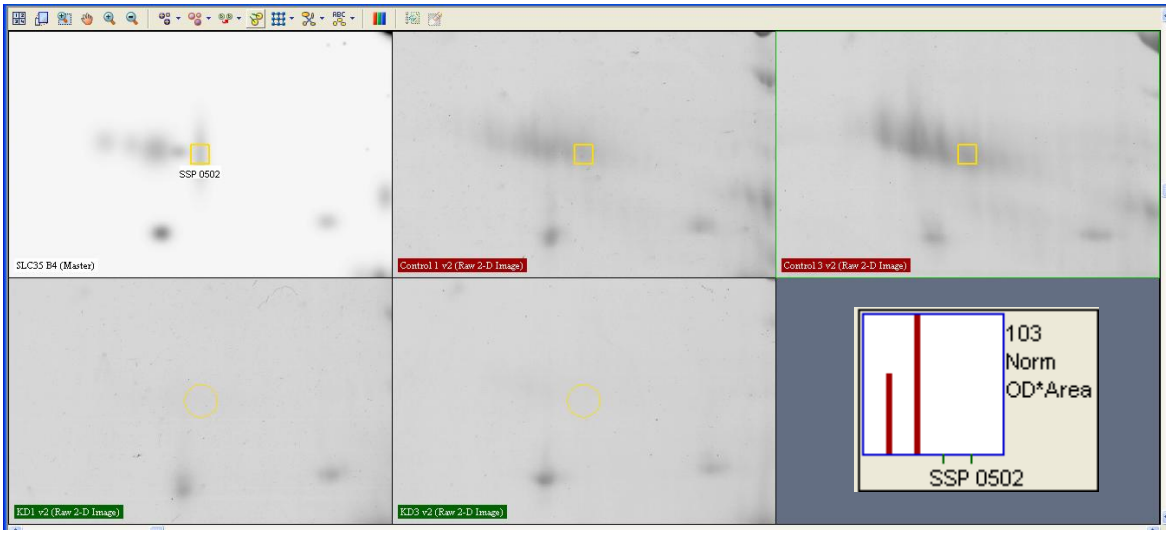

Fig. 3.25. Spot SSP 0502. Protein is completely under-expressed when comparing and averaging absorbance values for control gels as compared to knockdown gels of SLC35b4.

Spot SSP 1042 localized correctly in all 4 gels (although it should be noted that it is part of a protein cluster that was under-expressed, 3 in total: SSP 1042, 5401 and 2409) and is completely under-expressed as intensity values from KD gels are negligible leading to the conclusion that protein expression was totally inhibited (Figure 3.26).

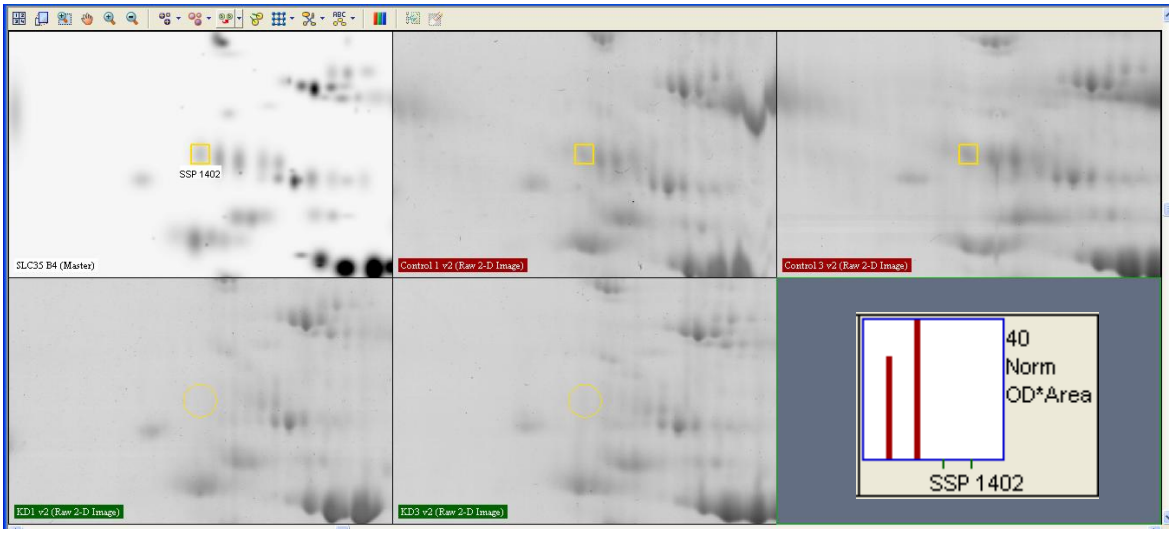

Fig. 3.26. Spot SSP 1042. Protein is completely under-expressed when comparing and averaging absorbance values for control gels as compared to knockdown gels of SLC35b4.

Spot SSP 2406 was localized correctly in all 4 gels (although it should be noted that it is part of a protein cluster that was under-expressed, 3 in total: SSP 1042, 5401 and 2409) and is completely under-expressed as intensity values from KD gels are negligible leading to the conclusion that protein expression was totally inhibited (Figure 3.27).

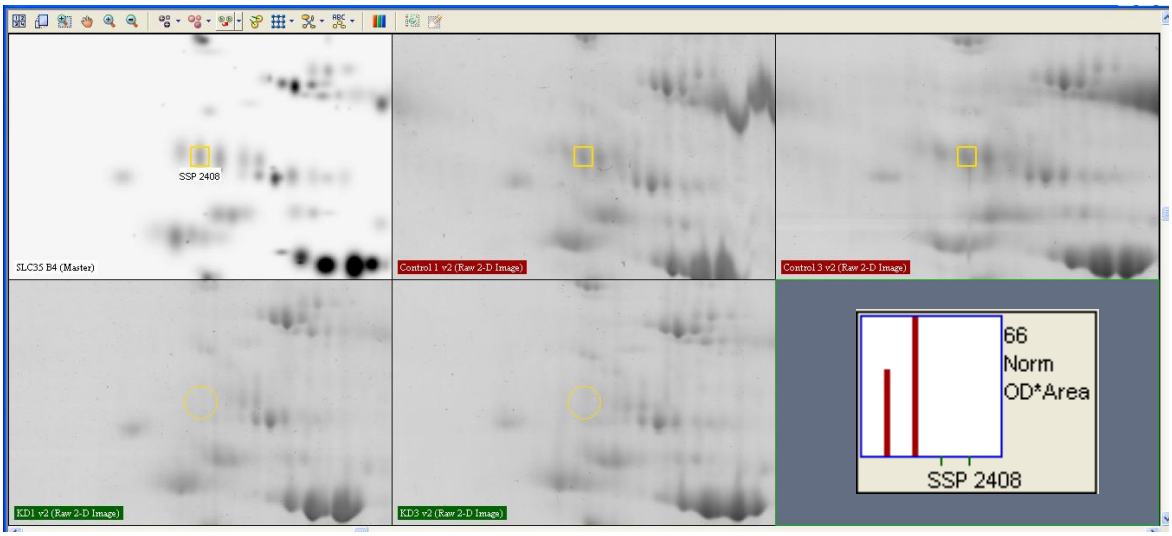

Fig. 3.27. Spot SSP 2406. Protein is completely under-expressed when comparing and averaging absorbance values for control gels as compared to knockdown gels of SLC35b4.

Spot SSP 5401 was localized correctly in all 4 gels (although it should be noted that it is part of a protein cluster that was under-expressed, 3 in total: SSP 1042, 5401 and 2409) and is completely under-expressed as intensity values from KD gels are negligible leading to the conclusion that protein expression was totally inhibited (Figure 3.28).

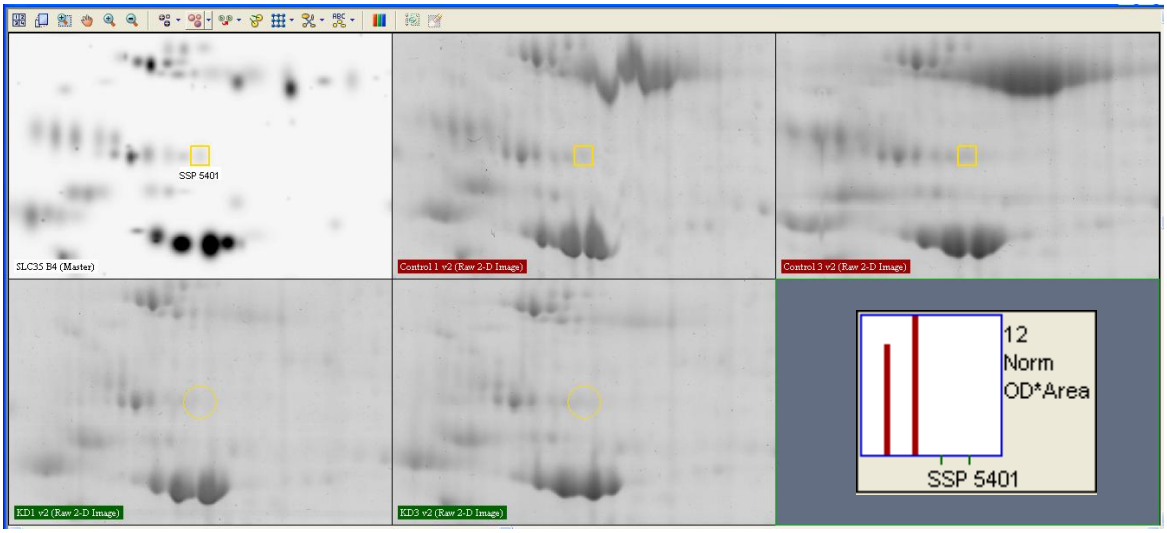

Fig. 3.28. Spot SSP 5401. Protein is completely under-expressed when comparing and averaging absorbance values for control gels as compared to knockdown gels of SLC35b4.

Spot SSP 6203 was localized correctly in all 4 gels and is over-expressed by 9.15 times as compared to the control gel (Figure 3.29). Manually averaging intensities of control gels and dividing by averaged intensities of KD gels determined relative expression.

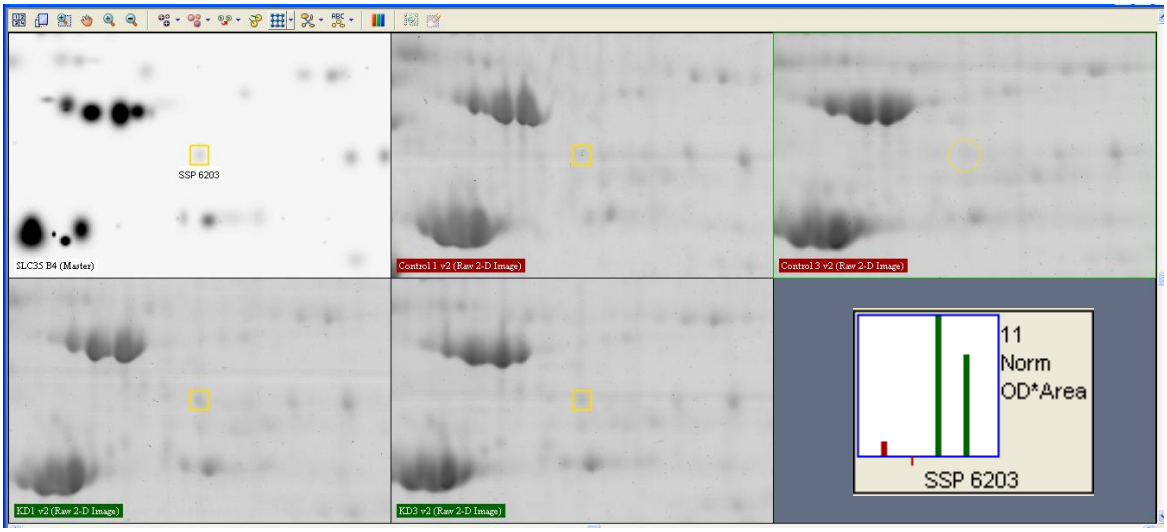

Fig. 3.29. Spot SSP 6203. Protein is over-expressed by 9.15 when comparing and averaging absorbance values for control gels as compared to knockdown gels of SLC35b4.

Using the 2D gels of Ctrl 1 and Ctrl 3 and plotting the log of the protein size (kDa) of the ladder versus the distance they travelled (cm) (Figure 3.30), a linear trend is apparent and may be used to calculate the size of the differentially expressed proteins.

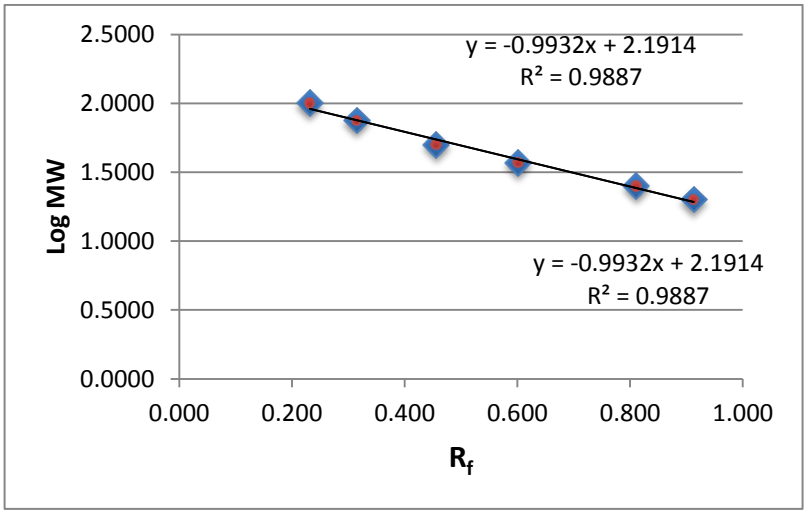

Figure 3.30. 2D standard curve of log of protein molecular weight (MW) vs. Ratio of Fronts (R_f)

Results of an estimation of both MW and pI from Ctrl 1 and Ctrl 3 2D gels are displayed in Table 3.8.

Table 3.8. Respective estimation of size and pI of differentially expressed proteins

Spot	pI	MW
SSP 502	4.6 ± 0.1	70.0 ± 0.2
SSP 6501	6.3 ± 0.1	70 ± 1
SSP 5401	6.05 ± 0.1	61.8 ± 0.6
SSP 6203	6.5 ± 0.0	50.34 ± 0.01
SSP 6204	6.5 ± 0.0	46.37 ± 0.03
SSP 8102	7.2 ± 0.0	42.01 ± 0.07
CLUSTER*	5.5 ± 0.1	64.4 ± 0.2

*The protein cluster mentioned in the table comprised the following spots: SSP 1402, SSP 2408, SSP 2406 and SSP 2409.

CHAPTER FOUR
DISCUSSION

4.1. One-Dimensional Electrophoresis Workflow:

4.1.1. Real-Time PCR

Using G6PDH (H6PD) as a reference gene, the relative expression of SLC35b4 in knockdown samples as calculated by the ΔCq method indicated a 58% decrease in expression (Figure 3.4). This is comparable to results obtained by Yazbek *et al.* (2011) who demonstrated a relative expression of >50% following KD of SLC35b4. In comparison though, Yazbek *et al.*. used the 18S rRNA as a reference gene. They also employed the ΔΔCq method.

4.1.2. One-Dimensional Gel Electrophoresis and Blotting (Western Blot)

Arias & Cartee (2005) were able to identify 8 bands, from liver protein, using the same primary antibody for O-glycosylated proteins that we used. Their study was aimed at identifying differentially expressed O-glycosylated proteins between calorie restricted (CR) and control group of mice. No effect of CR restriction was found on O-glycosylated proteins in liver. The study was intended to follow whether a previously described CR-induced decrease in hexosamines by Gazdag *et al.*. (2000) was accompanied by a change in protein O-glycosylation status in rat muscle and liver tissue (Arias & Cartee, 2005; Gazdag *et al.*, 2000).

Our study was able to identify 7 bands of O-glycosylated proteins from the HepG2 cell line (Liver hepatocellular carcinoma cells). Bands observed ranged in size from 35-270 kDa.

Following KD of SLC35b4, a subsequent western blot that compared between a control siRNA and the KD triplex siRNA revealed one differentially expressed protein between the 50 and 75 ladder markers. The expression of protein "X" was decreased by approximately 65% as compared to control

siRNA. When matching the approximate protein size with possible glycosylated proteins in the insulin resistance pathway, Protein Kinase B (Akt) is the most likely candidate.

After replacing for the unknown (x) in the trendline of standard curve (Figure 3.8), the size of protein X was determined to be 67.5 kDa. This does not match any of the glycosylated proteins in the insulin resistance pathway but may indicate a protein downstream or upstream of the pathways perhaps.

4.1.3. Matrix-Assisted Laser Desorption Ionization - Time of Flight (MALDI-TOF)

As mentioned in the results section 3.2.5, we were unable to identify the differentially expressed protein "X" by MALDI using protocols, referred to as Blotting and Removal of Nitrocellulose (BARN), by Luque-Garcia *et al.*. (2006, 2008). We attempted identification of protein "X" Peptide Mass Fingerprinting (PMF), however, the identification was not possible for the following reasons:

- Both protocols used soluble (myoglobin and BSA) and membrane (uroplakins II and III) proteins that only contained 3-4 proteins/well on the 1D SDS-PAGE, this in turn resulted in the transfer of a 3-4 protein/well to the nitrocellulose membrane
    - Since we were running total protein lysate, cutting and identification of one band would actually entail the identification of several proteins at once.
    - Also, stripping of the membrane from primary and secondary antibodies failed repeatedly (which is why we resorted to the 2 overlapping membranes for Actin probing). The antibodies are of high molecular weight and would cause interference (a higher signal) than any other protein to be identified.
- Luque-Garcia's *et al.*. (2006, 2008) protocol suggested the use of a non-protein based blocking buffer following the transfer to nitrocellulose membrane. We were not able to procure such a buffer and blocking was done using 1% non-fat milk that in itself contains a variety of proteins which could mask the signal of proteins to be identified.

4.2. Two-Dimensional Electrophoresis Workflow:

4.2.1. SYBR Green Real-Time PCR

Although real-time results indicated no significant change of gene expression for KD 1 with respect to Control 1, and no significant change of gene expression of KD 2 with respect to Control 2, the differentially expressed proteins from the 2 KD gels as compared to the 2 Control gels verify the knockdown using the tri-silencer siRNA.

A study by Holmes *et al.* (2010), describes a phenomenon that gives rise to false negatives when validating a KD using real-time PCR. Their data suggests that for certain mRNAs, degradation of the 3' mRNA fragment leaves an mRNA fragment that can act as a template for cDNA synthesis, giving rise to false negative results and the rejection of a valid siRNA duplex. They show that careful design of RT-qPCR primers in such a way to avoid the above-mentioned phenomenon is possible and compare to validation by western blot (Holmes *et al.*., 2010).

4.2.2. Two-Dimensional Gel Electrophoresis

It is estimated that 50% of all proteins are glycosylated, and among the currently known Post Translational Modifications (PTMs), glycosylation has been widely recognized as one of the most influential parameters in the alteration of protein 2-dimensional electrophoresis (2-DE) patterns. This modification alters the apparent molecular weight of a protein, and when charged monosaccharides, such as sialic acids or sulphated monosaccharides, are added to N or O-glycan chains, the pI of the protein is also changed. (Zhang & Williamson, 2005; Barrabés *et al.*., 2010).

When the 1D workflow was halted by the fact that we were not able to identify the differentially expressed protein, 2D electrophoresis was the next step in attempting to identify the effect of SLC35b4 knockdown.

The estimated size of the differentially expressed proteins was determined by plotting the log of molecular weight of ladder proteins versus the R_f value

(Figure 4.2). The graph exhibited a linear trend. Since only two data points were available per protein, separate standard curves were generated from gels of Control 1 and Control 3, a linear fit applied and the molecular weight of the proteins computed. The values were then averaged and standard deviation calculated. The standard curves are shown in Figure 4.3 and the results are summarized in Table 4.1.

Also, protein Isoelectric points were determined by dividing the gel in a linear manner from 3-10 (pH) since the strip's gel assumes a linear graduation from pH 3 to pH 10. A similar technique was followed by Wilson *et al.* (2002), where they estimated pI based on linear pI gradient measurement from the 1st dimension strip and then compared values to actual protein MW and pI after identification through mass spectrometry (Wilson *et al.*., 2002).

Identification of differentially expressed proteins is a must before suggestion the possible role of the KD of the SLC35b4 receptor in the insulin resistance pathway (on both O-glycosylated and non O-glycosylated proteins).

Interestingly however, all of the over-expressed proteins (3) have very close matches in molecular weight (Table 4.1) to O-glycosylated proteins of the IR pathway mentioned in Table 1.1.

Table 4.1. Possible matches of proteins in the IR pathway O-glycosylated proteins showing that 3 spots' molecular weight match some protein in the pathway.

O-glycosylated proteins of Insulin receptor pathway	MW	Proposed match from differentially expressed proteins
IRS	135 kDa	--
PI3K	43 kDa	SSP 8102 (MW= 42.01 ± 0.07 kDa)
PDK1	49 kDa	SSP 6203 (MW= 50.34 ± 0.01 kDa)
Akt	55 kDa	--
Mun18-c	45 kDa	--
GSK3β	46 kDa	SSP 6204 (MW= 46.37 ± 0.03 kDa)
AMPK	30 kDa	--
SP1	83 kDa	--
IR	156 kDa	--

In conclusion, although this study was not able to identify the 10 differentially expressed proteins between the knockdown and control gels of SLC35b4, but it was able to optimize the 2-DE method needed to do so. Thus, future work needs to validate the knockdown of SLC35b4 using the SYBR green Real-Time PCR, and this may be done by designing new primers that would not result in the false negative result that was obtained. Also, since all differentially expressed proteins fell in the 4-7 isoelectric point range, it would also be beneficial to repeat the 2D electrophoresis on 4-7 pH strips and consequently obtained a better resolution. Finally, to assess the role of SLC35b4 in insulin resistance using its knockdown, it is imperative to identify the differentially expressed proteins using mass spectrometry and then proceed with pathway analysis.

CHAPTER FIVE
CONCLUSIONS

- Western blot analysis showed one differentially expressed O-glycosylated protein in a HepG2 cell line knockdown of SLC35b4

- Size of differentially expressed protein "X" was determined to be approximately 67.46 kDa

- Two dimensional electrophoresis study of SLC35b4 knockdown resulted in:
  - The differential expression of 10 proteins, more than 2 fold, as compared to control siRNA
  - Three proteins were determined to be over-expressed as compared to control
  - Seven proteins were determined to be under-expressed as compare to control
  - The estimation of MW and pI of these 10 differentially expressed proteins
  - Three of the differentially expressed proteins (corresponding to Spots SSP 6203, 6204 and 8102) have very close matches in O-glycosylated proteins of the insulin resistance pathway where O-glycosylation might play a role in glucose synthesis

- Identification of differentially expressed protein is a must in order to assess SLC35b4 role in the IR pathway using its knockdown

BIBLIOGRAPHY

Altshuler, D., Daly, M. & Lander, E. (2008). Genetic mapping in human disease. *Science, 322*, 881-888.

Alwan, A., Maclean, D.R., Riley, L.M., d'Espaignet, E.T., Mathers, C.D., Stevens, G.A. & Bettcher, D. (2010). Monitoring and surveillance of chronic noncommunicable diseases: Progress and capacity in high-burden countries. *The Lancet*, *376,* 1861-1868.

Arias, E. & Cartee, G. (2005). Relationship between protein O-linked glycosylation and insulin-stimulated glucose transport in rat skeletal muscle following calorie restriction or exposure to O-(2-acetamido-2-deoxy-d-glucopyranosylidene)amino-N-phenylcarbamate. *Acta Physiologica Scandinavica, 183*(3), 281-289.

Arya, R., Blangero, J., Williams, K., Almasy, L., Dyer, T.D., Leach, R.J. … Duggirala, R. (2002). Factors of insulin resistance syndrome--related phenotypes are linked to genetic locations on chromosomes 6 and 7 in nondiabetic mexican-americans. *Diabetes, 51*(3), 841-847.

Ashikov, A., Routier, F., Fuhlrott, J., Helmus, Y., Wild, M., Gerardy-Schahn, R. & Bakker, H. (2005). The human solute carrier gene SLC35B4 encodes a bifunctional nucleotide sugar transporter with specificity for UDPxylose and UDP-N-acetylglucosamine. *Journal of Biological Chemistry, 280,* 27230-27235.

Bakker, H., Oka, T., Ashikov, A., Yadav, A., Berger, M., Rana, N.A., … Gerardy-Schahn, R. (2009). Functional UDP-xylose transport across the endoplasmic reticulum/Golgi membrane in a Chinese hamster ovary cell mutant defective in UDP-xylose Synthase. *Journal of Biological Chemistry, 284*(4), 2576-2583.

Barrabés, S., Sarrats, A., Fort, E., De Llorens, R., Rudd, P.M. & Peracaula, R. (2010). Effect of sialic acid content on glycoprotein pI analyzed by two-dimensional electrophoresis. *Eletrophoresis, 31*(17), 2903-2912.

Billings, L. & Jose, F. (2010). The genetics of type 2 diabetes: What have we learned from GWAS? *Annals of the New York Academy of Sciences, 1212*(1), 59-77.

Buse, M.G. (2006). Hexosamines, insulin resistance, and the complications of diabetes: Current status. *American Journal of Physiology - Endocrinology and Metabolism, 290*(1), E1-E8.

Dentin, R., Hedrick, S., Xie, J., Yates, J. 3rd & Montminy, M. (2008). Hepatic glucose sensing via the CREB coactivator CRTC2. *Science, 319*(5868), 1402-1405.

Feitosa, M.F., Borecki, I.B., Rich, S.S., Arnett, D.K., Sholinsky, P., Myers, R.H. … Province, M.A. (2002). Quantitative-trait loci influencing body-mass index reside on chromosomes 7 and 13: The National Heart, Lung, and Blood Institute Family Heart Study. *American Journal of Human Genetics, 70*(1), 72-82.

Fox, C.S., Heard-Costa, N., Cupples, L.A., Dupuis, J., Vasan, R.S. & Atwood, L.D. (2007). Genome-wide association to body mass index and waist circumference: The Framingham Heart Study 100K project. *BMC Medical Genetics, 8*(Suppl 1), S18.

Freeman, H. & Cox, R. (2006). Type-2 diabetes: A cocktail of genetic discovery. *Human Molecular Genetics, 15* (suppl 2), R202-R209.

Friedman, D.B., Hoving, S. & Westermeier, R. (2009). Isoelectric focusing and two-dimensional gel electrophoresis. *Methods in Enzymology, 463,* 515-540.

Gazdag, A.C., Wetter, T.J., Davidson, R.T., Robinson, K.A., Buse, M.G., Yee, A.J., … Cartee, G.D. (2000). Lower calorie intake enhances muscle insulin action and

reduces hexosamine levels. *American Journal of Physiology - Regulatory, Integrative and Comparative Physiology, 278*(2), R504-12.

Hanisch, F.G. (2011). Top-down sequencing of O-glycoproteins by in-source decay matrix-assisted laser desorption ionization mass spectrometry for glycosylation site analysis. *Analytical Chemistry, 83*(12), 4829-4837.

Hanover, J., Krause, M. & Love, D. (2010). The hexosamine signaling pathway: O-GlcNAc cycling in feast or famine. *Biochimica et Biophysica Acta, 1800*(2), 80-95.

Hase, S., Kawabata, S., Nishimura, H., Takeya, H., Sueyoshi, T., Miyata, T., … Ikenaka, T. (1988). A new trisaccharide sugar chain linked to a serine residue in bovine blood coagulation factors VII and IX. *Journal of Biochemistry, 104*(6), 867-868.

Hirbli, K.I., Jambeine, M.A., Slim, H.B., Barakat, W.M., Habis, R.J. & Francis, Z.M. (2005). Prevalence of diabetes in greater Beirut. *Diabetes Care, 28*(5), 1262.

Holmes, K., Williams, C.M., Chapman, E.A. & Cross, M.J. (2010). Detection of siRNA induced mRNA silencing by RT-qPCR: Considerations for experimental design. *BioMed Central Research Notes*, *3,* 53.

Karthik, D., Ilavenil, S., Kaleeswaran, B., Sunil, S. & Ravikumar, S. (2012). Proteomic analysis of plasma proteins in diabetic rats by 2D electrophoresis and MALDI-TOF-MS. *Applied Biochemistry and Biotechnology, 166*(6), 1507-1519.

Laramie, J.M., Wilk, J.B., Williamson, S.L., Nagle, M.W., Latourelle, J.C., Tobin, J.E., … Myers, R.H. (2008). Polymorphisms near EXOC4 and LRGUK on chromosome 7q32 are associated with Type 2 Diabetes and fasting glucose; the NHLBI Family Heart Study. *BMC Medical Genetics, 22*(9), 46.

Lay, J.O. Jr & Holland, R.D. (2000). Rapid identification of bacteria based on spectral patterns using MALDI-TOFMS. *Methods in Molecular Biology, 146,* 461-487.

Lefebvre, T., Dehennaut, V., Guinez, C., Olivier, S., Drougat, L., Mir, A.M.… Michalski, J.C. (2010). Dysregulation of the nutrient/stress sensor O-GlcNAcylation is involved in the etiology of cardiovascular disorders, type-2 diabetes and Alzheimer's disease. *Biochimica et Biophysica Acta*, *1800*(2), 67-79.

Li, W.D., Li, D., Wang, S., Zhang, S., Zhao, H. & Price, R.A. (2003). Linkage and linkage disequilibrium mapping of genes influencing human obesity in chromosome region 7q22.1-7q35. *Diabetes, 52*(6), 1557-1561.

Lippincott, W. (2007). Understanding diabetes mellitus: Causes and pathophysiology. In Lippincott Williams & Wilkins. (Ed.), *Diabetes mellitus: A guide to patient care* (pp. 15). Philadelphia: Wolters Kluwer.

Love, D. & Hanover, J. (2005). The hexosamine signaling pathway: Deciphering the "O-GlcNAc code". *Science STKE, 29*(312), re13.

MacPhee, D.J. (2010). Methodological considerations for improving Western blot analysis. *Journal of Pharmacological and Toxicological Methods, 61*(2),171-177.

Marko-Varga, G. (2005). Pathway proteomics: Global and focused approaches. *American Journal of Pharmacogenomics, 5*(2), 113-122.

Marvin, L.F., Roberts, M.A. & Fay, L.B. (2003). Matrix-assisted laser desorption/ionization time-of-flight mass spectrometry in clinical chemistry. *Clinica Chimica Acta, 337*(1-2), 11-21.

Masharani, U. & German, M.S. (2011). Pancreatic hormones and diabetes mellitus. In D. Shoback & D.G. Gardner (Eds.), *Greenspan's basic & clinical endocrinology* (9th ed, pp.121). New York: McGraw-Hill Medical.

Maszczak-Seneczko, D., Olczak, T. & Olczak, M. (2011). Subcellular localization of UDP-GlcNAc, UDP-Gal and SLC35B4 transporters. *Acta Biochimica Polonica, 58*(3), 413-419.

McClain, D.A., Lubas, W.A., Cooksey, R.C., Hazel, M., Parker, G.J., Love, D.C. & Hanover, J.A. (2002). Altered glycan-dependent signaling induces insulin resistance and hyperleptinemia. *Proceedings of the National Academy of Sciences, 99*(16), 10695-10699.

Melmed, S., Polonsky, K.S., Larsen, P.R. & Kronenberg, H.M. (2011). Type II diabetes mellitus: Pathophysiology. In S. Melmed, K.S. Polonsky, P.R. Larsen & H.M. Kronenberg (Eds.), *Williams textbook of endocrinology* (12th ed, pp.93). Philadelphia: Elsevier/Saunders.

Moloney, D.J., Shair, L.H., Lu, F.M., Xia, J., Locke, R., Matta, K.L. & Haltiwanger, R.S. (2000). Mammalian Notch1 is modified with two unusual forms of O-linked glycosylation found on epidermal growth factor-like modules. *Journal of Biological Chemistry, 275*(13), 9604-9611.

Moriarity, J.L., Hurt, K.J., Resnick, A.C., Storm, P.B., Laroy, W., Schnaar, R.L. & Snyder, S.H. (2002). UDP-glucuronate decarboxylase, a key enzyme in proteoglycan synthesis: Cloning, characterization, and localization. *Journal of Biological Chemistry, 277*(19),16968-16975.

Nathan, D.M., Buse, J.B., Davidson, M.B., Ferrannini, E., Holman, R.R., Sherwin, R., …European Association for Study of Diabetes. (2009). Medical management of hyperglycemia in type 2 diabetes: A consensus algorithm for the initiation and adjustment of therapy. *Diabetes Care, 32*(1), 193-203.

Sage, A.T., Walter, L.A., Shi, Y., Khan, M.I., Kaneto, H., Capretta, A. & Werstuck, G.H. (2010). Hexosamine biosynthesis pathway flux promotes endoplasmic reticulum stress, lipid accumulation, and inflammatory gene expression in hepatic cells. *American Journal of Physiology - Endocrinology and Metabolism, 298*(3), E499-511.

Saunders, C.L., Chiodini, B.D., Sham, P., Lewis, C.M., Abkevich, V., Adeyemo, A.A., … Collier, D.A. (2007). Meta-analysis of genome-wide linkage studies in BMI and obesity. *Obesity (Silver Spring), 15*(9), 2263-2275.

Seidler, J., Zinn, N., Boehm, M.E., Lehmann, W.D. (2010). De novo sequencing of peptides by MS/MS. *Proteomics, 10*(4), 634-649.

Shivashankar, M. & Mani, D. (2011). A brief overview of diabetes. *International Journal of Pharmacy and Pharmaceutical Sciences, 3*(4), 22-27.

Tang, W., Miller, M.B., Rich, S.S., North, K.E., Pankow, J.S., Borecki, I.B., … Arnett, D.K. (2003). Linkage analysis of a composite factor for the multiple metabolic syndrome: The National Heart, Lung, and Blood Institute Family Heart Study. *Diabetes, 52*(11), 2840-2847.

Tarik, I. & MeiShiue, K. (2008). O-GlcNAc modification of transcription factors, glucose sensing and glucotoxicity. *Trends in Endocrinology and Metabolism, 19*(10), 380-389.

Teo, C.F., Wollaston-Hayden, E.E. & Wells, L. (2010). Hexosamine flux, the O-GlcNAc modification, and the development of insulin resistance in adipocytes. *Molecular Cell Endocrinology, 318*(1-2), 44-53.

Towbin, H., Staehelin, T. & Gordon, J. (1979). Electrophoretic transfer of proteins from polyacrylamide gels to nitrocellulose sheets: Procedure and some applications. *Proceedings of the National Academy of Sciences, 76*(9), 4350-4354.

Wang, H., Julenius, K., Hryhorenko, J. & Hagen, F.K. (2007). Systematic analysis of proteoglycan modification sites in *Caenorhabditis elegans* by scanning mutagenesis. *Journal of Biological Chemistry, 282*(19), 14586-14597.

Westermeier, R. & Schickle, H. (2009). The current state of the art in high-resolution two-dimensional electrophoresis. *Archives of Physiology and Biochemistry, 115*(5), 279-285.

Wheeler, E. & Barroso, I. (2011). Genome-wide association studies and type 2 diabetes. *Briefings in Functional Genomics, 10*(2), 52-60.

Wilson, N.L., Schulz, B.L., Karlsson, N.G. & Packer, N.H. (2002). Sequential analysis of N- and O-linked glycosylation of 2D-PAGE separated glycoprotein. *Journal of Proteome Research*, *1*, 521-529.

Wilson, N., Simpson, R. & Cooper-Liddell, C. (2009). Introductory glycosylation analysis using SDS-PAGE and peptide mass fingerprinting. *Methods* in *Molecular Biology*, *534*, 205-212.

Yang, X., Ongusaha, P.P., Miles, P.D., Havstad, J.C., Zhang, F., So, W.V., … Evans, R.M. (2008). Phosphoinositide signalling links O-GlcNAc transferase to insulin resistance. *Nature, 451*(7181), 964-969.

Yazbek, S.N., Buchner, D.A., Geisinger, J.M., Burrage, L.C., Spiezio, S.H., Zentner, G.E., … Nadeau, J.H. (2011). Deep congenic analysis identifies many strong, context-dependent QTLs, one of which, Slc35b4, regulates obesity and glucose homeostasis. *Genome Research, 21,* 1065-1073.

Zhang, S. & Williamson, B.L. (2005). Characterization of protein glycosylation using chip-based nanoelectrospray with precursor ion scanning quadrupole linear ion trap mass spectrometry. *Journal of Biomolecular Techniques, 16*(3), 209-219.